INVESTIGATIONS OF THE REDOX KINETICS OF CONDUCTING POLYMERS

Dissertation
zur
Erlangung des Doktorgrades
der Mathematisch-Naturwissenschaftlichen Fakultät
der Christian-Albrechts-Universität
zu Kiel

vorgelegt von

Evgenij Barsoukov

Kiel 1996

Table of Contents

1 Introduction

A new exiting branch of electrochemistry was born in 1977, as Heeger & McDiarmid [*1*] discovered the ability of polyaromatics with conjugated double bonds to undergo chemical and electrochemical redox transitions to yield polymers with high electronic conductivity. The simple electrochemical technique of producing conducting polymer layers was first reported by Diaz et al. [*2*] in 1979. After that, conducting polymers have become a beloved object of investigation by electrochemists. Many proposals for possible applications of these materials have been put forward in the last few years because of their unique electronic, electrochemical and optical properties. Some of these include their use in storage batteries [*3*], electrochromic displays [*4*] and sensors [*5*]. However, no extensive commercialization of any of these systems has been observed up to the present. This can be partially accounted for their very complex chemical and physical behaviors. The price paid for the simplicity of their electrochemical preparation is the high complexity of the structure and properties of the obtained polymer layers. For such applications as supercapacitors or electrochromic devices, thin films of polymer on the electrode are required, however preparation of such films by use of chemically synthesized polymers would be connected with unreasonable expenses. Hence, the understanding of the electrochemical kinetics in view of polymer layer properties is decisive for the future use of conducting polymers.

A large number of different processes influence the kinetics of the recharge of electrochemically synthesized conducting polymers, however a couple of processes is common to most of them. These are: charge transfer through the polymer and the electrolyte, included in the polymer layer; transport of counterions into the polymer matrix; formation of double layer on the polymer interface; establishment of chemical and membrane equilibrium and the associated structural changes. Practically all kinds of existing physical and chemical methods have been used to investigate the properties of conducting polymers. Investigations have been performed under potentiostatic control by cyclic voltammetry along with other measurement techniques, such as electrochemical impedance spectroscopy (EIS) [*6- 9*], conductivity measurements

[*10- 12*], ESR [12], quartz microbalance [*13*], uv-vis spectroscopy [*14*] etc. Results of current pulse experiments under galvanostatic control have also been reported [*7*,*15*,*16*]. However, due to complexity of the electrochemical behavior of conducting polymers, much questions remain still open.

- Due to the manifold of processes, determining the behavior of conducting polymers, the cyclic voltammetry is not able to give their physical and chemical parameters directly. One of the commonly admitted features of the cyclic voltammograms (CVs) of conducting polymers is its strong capacitive character in potential range, where polymer is in an oxidized form [*17-20*]. Several attempts have been made to describe such a behavior of coated with conducting polymer electrodes [9,*21-26*]. Feldberg [21] assumed that the capacitance is proportional to the amount of oxidized polymer but is independent of the electrode potential once the polymer film has been converted into its oxidized form. White and coworkers [22,23] extended the approach of Feldberg, taking into account the porosity of the polymer films. Kaplin and Qutubuddin [24] simulated charge transfer during switching of conducting polymers for both the reversible and the irreversible cases, but neglected the capacitive effects.

The combined analysis of the cyclic voltammograms and data obtained by measurements from a different source, can allow to exclude one of the processes, effecting the current response during the potential sweep and therefore to simplify the investigation significantly. Tanguy and coworkers measured the impedance of chemically synthesized polypyrrole [25] and of electrodes covered with 3-methylthiophene [9] over a large frequency range for different values of the electrode potential. They measured electrochemical impedance spectra in steady state and calculated the capacitive part of the current as $I_c = C(U)(dU/dt)$ where: C(U) is an expression for the voltage dependence of the capacitance obtained by fitting of the low frequency part of experimental impedance data and dV/dt is the sweep rate. Use of steady state impedance data for predicting CVs requires consideration of pseudoequlibrium conditions during the potential cycle. Cyclic voltammograms with different scan rates performed on polybithiophene films do not prove this assumption. Impedance spectra measured at a particular potential are dependent on the rate of potential scan. Therefore, the attempt has been made, to predict CVs using the

resistance and capacity values evaluated from impedance spectra, which were measured *during* potential sweep with a respective scan rate (chapter 4.1). Current response was calculated by a numerical solution of a differential equation considering both C and R values dependent on the applied electrode potential.

- The model of serial connected capacitance and resistance is only usable to describe the slow recharge of conducting polymers. In the intermediate frequency range, corresponding to fast processes in the time domain, the porous nature of electrochemically deposited polymer layer has to be taken into account. Due to porosity, the polymer-electrolyte interface resides not only on the geometrically edge of the layer but also inside of it. Different inner interfaces become nonequipotential during the current flow through the layer. The analysis of alternating current (ac) response allows us to evaluate the resistance of polymer layer, however, the path of current flow by conventionally impedance measurements travels through the pores, filled with electrolyte, as well as through the compact polymer aggregates. Hence, the electronic conductivity of polymer becomes indistinguishable from the ionic conductivity of electrolyte. An analysis of experimental impedance spectra of polymers in conducting state shows, that the contribution of one of the two possible resistances can be neglected and does not have considerable effect [*27*]. The question remains open though, as to which one is it. Measurements, where the charge transfer does not cross the polymer-electrolyte interface can allow independent evaluation of one of the resistances. Several experimental designs for performing such experiments have been reported [5,11, *28-31*]. Paul et al. [5] have investigated the conductivity properties of polyaniline, electrochemically deposited onto an Au microelectrode array. The resistance was measured between two microelectrodes, spaced 1.7 μm apart. Schiavon et al. [*28*], Holze and Lippe [11], and Kankare and Kupila [29] have used a simpler, twin electrode configuration with two metal stripes separated by a gap a few micrometers wide, exposed to the electrolyte. The gap was bridged with a polymer layer through electrochemical deposition. The resistance measurement has been performed by applying a small dc voltage [11,28] or a 130 Hz ac voltage [29] to the electrodes across the gap. The 4-probe technique has also been successfully applied to in situ conductivity measurements on polymer covered electrodes by Olmedo et al. [31].

Measurement with a polymer layer, which is only contacted at the polymer or electrolyte side, could give resistance data along with other information, relevant to recharge kinetic, if performed within a wide frequency range. A new technique for multifrequency EIS measurements in the surface layer, nearly described in chapter 4.2, has been developed for this purpose. The technique has been applied to a twin-working electrode, bridged with electrochemically deposited polybithiophene. Measurements, both time-resolved in situ EIS during electrochemical deposition of polybithiophene and potential-resolved during oxidation/reduction potential sweeps, have been performed. The analysis of the electric field taking place in the electrode configuration used has allowed to make an estimation for the specific electronic resistance and the polymer layer thickness.

- As mentioned above, the structure of electrochemically deposited polymer layer highly depends on the condition of preparation and considerably influences the recharge behavior of the conducting polymer. The deposition of conducting polymers onto metal electrodes during electrochemical polymerization from monomer containing electrolytes is a rather complex process involving diffusion of monomer to the electrode surface and electrooxidation, subsequent back diffusion, oligomerization, and precipitation onto the electrode. Hillman and coworkers [32,14] suggested a deposition mechanism including instantaneous nucleation, followed by 3-D growth of the nuclei until they overlap leading to formation of a plain polymer layer, but Li and Albery [33] have pointed out that the alternative 2-D growth mechanism is also possible. Investigations of the electrochemical polymerization of thiophene and its derivatives have been performed by potential pulse [32,33] and potential sweep [34-36] techniques combined with other measurement techniques, such as ellipsometry [36-38], conductivity measurements [29,39,40], quartz microbalance [41,42], uv-vis spectroscopy [32], EIS [43], etc. Measurements upon galvanostatic conditions can be very useful for the study of the early stages of polymer deposition, where formation rate of polymer layer can be controlled according to the requirements of an impedance experiment.

Investigation of thickness dependence of impedance spectra can be easily performed *in situ,* without removing the polymer coated electrode from the monomer containing

electrolyte, by setting a zero current after deposition of every new layer. While galvanostatic methods were used earlier predominantly for preparation of polymer films and for proving their charge/discharge cyclability performance [44-47], a new technique of EIS measurements, using the advantages of the galvanostatical condition, has been developed. EIS measurements, aimed to investigate the process of electrochemical growth of polybithiophene and the dependence of impedance spectra on the layer thickness, have been performed as closely described in chapter 4.3. Time resolved impedance spectra have been measured *in situ* during current controlled polymerization. Thus the polymer film formation could be traced out for a wide range of electric charge passed, i.e. from the onset of polymer deposition until a relatively thick layer was grown. The impedance spectra obtained has been analyzed using models of Ho et al. [48] and Paasch et al. [27], and the suitability of both models for analysis of layers with different thickness has been discussed.

- The simple model [6], based on the work of Ho and coworkers [48], considers a homogeneous nonporous polymer layer and can thus only be used for very thin layers. Impedance measurements on polymer layers of different thicknesses, made by Tanguy [9] as well as measurements made in this work let conclude, that transport of dopants during recharge is not hindered in the bulk of polymer layer but in the polymer aggregates, which are relatively small in comparison to the layer thickness. A polymer layer can thus be imagined as a 2-phase medium, where one phase consist of the polymer aggregates and another the electrolyte, which fills the cavities between them. A mathematical model describing electrochemical behavior of such polymer layer is developed by Paasch et al. [27]. A good correspondence of experimental results to this model was observed during the investigation of oxidized polybithiophene layers with different thicknesses. However, the assumption of macrohomoheneity in direction perpendicular to the electrode interface was made, which is not strictly fulfilled by most of electrochemically prepared polymer layers. Discrepancies between experimental and simulated spectra were not considerable for polymer in oxidized state. Macroinhomogeneity of specific resistance does not affect the spectra because of the small value, which resistance of an oxidized polymer exhibits nonetheless. The situation change in case of reduced polymer, where experimental data can not be described by this model any further. To analyze experimental data measured on polymer layers in

reduced state, the model of Paasch has been extended for the case of inhomogenenous polymer layers (chapter 4.4). EIS measurements on polybithiophene layers were performed steady state at different electrode potentials and the experimental result were analyzed using the developed model.

2 Experimental

2.1 Electronic equipment

All measurements described in this thesis have been performed using a computer operated fast potentiostat/galvanostat, developed in our working group [*xlix*]. The normally used measurement design is shown below.

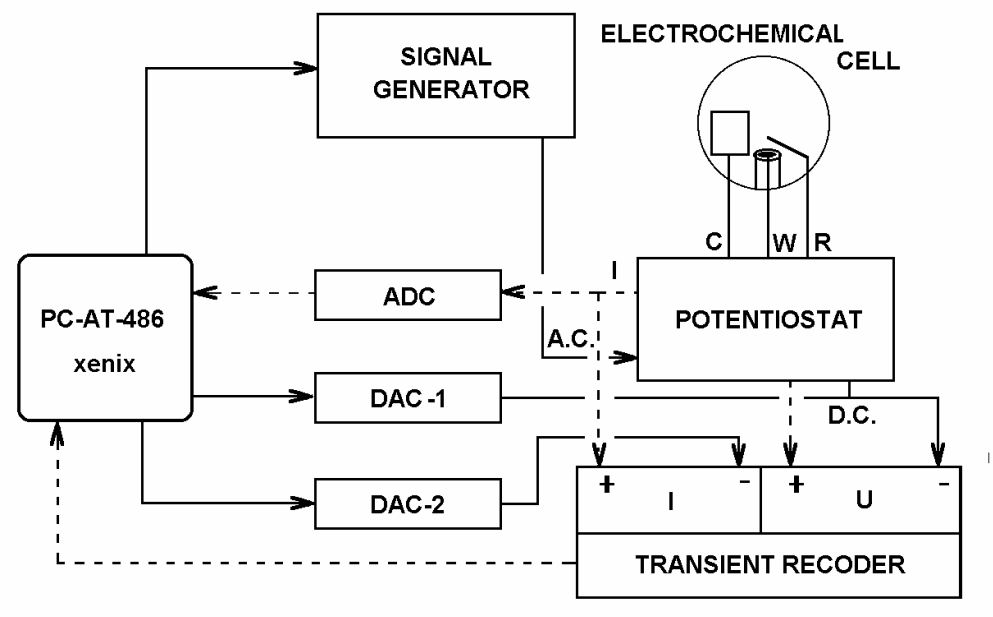

Fig. 1 Electronic design used for electric measurements, dashed lines - output signal routing, normal lines- input signal routing.

The characteristics of electronic devices, presented in Fig. 1, are listed in detail in the following table:

Fast potentiostat, Inst. f. Phys. Chem. University of Kiel	d.c. - 100 kHz
Signal generator, Inst. f. Phys. Chem. University of Kiel	• Perturbation signal burned in EPROM • DAC - 16 bit, synchronized with the transient recorder • 2×low pass filters, Kemo LTD Beckenham Kent, type VBF8
Transient recorder, Inst. f. Phys. Chem. University of Kiel	• 2×differential amplifiers • 2×low pass filters, Stanford Research Systems, inc. model SR640 • 2×ADC - 12 bit, 3 μs • 2×256 Kbytes record length
ADC, DAC-1, DAC-2, Inst. f. Phys. Chem. University of Kiel	12 bit, 3 μs
AT-486	16 Mbytes RAM, 256 Kbytes cache, XENIX

2.1.1 Conventional electrochemical techniques

CV, coulometry, potential- and current pulse experiments were carried out using the simplified electronic design shown in Fig. 1. Potentiostat/galvanostat was operated by signal of DAC-1, which was controlled by the computer. Output signal was filtered by a low pass filter, digitized by ADC and recorded. Software running under DOS and XENIX were used to operate and record the measurements. For especially exact low current measurements an extern DC-standard (Knick Berlin37 type S13) was used for operating of the galvanostat.

2.1.2 Impedance measurements

In situ FFT- impedance measurements were performed using the electronic equipment [xlix], shown in Fig. 1. In case of potentiostatic EIS measurements, the bias potential given by DAC-1 was overlaid by an alternating voltage signal, produced by the signal generator. A sum of 52 sinus waves, were burned into EPROM and used for generation of the perturbation signal in the frequency ranges shown below.

- 4 Hz- 30 kHz (τ=10 μs).
- 0.15 Hz- 5 kHz (τ=100 μs).
- 0.015 Hz - 450 Hz (τ=1000 μs).

Peak signal amplitude was selected specially for each particular measurement and never exceed 15 mV, so linear conditions for EIS could be provided. Alternating potential and current output signals were subtracted from the d.c. - bias component by differential amplifiers, filtered by a low pass filter to prevent aliasing effects, digitized and recorded by a two channel transient recorder. The perturbation signal was applied twice and only the second half of the signal was recorded to prevent transient effects. Information interchange between transient recorder and computer was initiated after each measurement. Recorded signal in time domain was transformed into frequency domain by means of fast Fourier transformation (FFT) immediately after each measurement or stored in RAM and analyzed after finishing the entire experiment. In some cases the „window“ method [*l*], using Hanning weighing function, was applied to additionally improve the impedance spectra quality. Amplitude spectra of potential and current signals were analyzed to prove the validity of measurements.

Measurement under galvanostatical conditions was performed analogously with the difference, that the operating signals were given on the input of galvanostat and resulting potential signals were recorded. The measurement equipment and data analysis are detailed described in [43].

2.1.3 Impedance measurements on the twin electrode

Measurement set-up used for EIS- measurements on the twin electrode was described in detail earlier [*li*]. It consisted of an FFT impedance spectrometer and a fast potentiostat connected to the electrochemical cell as shown in Fig. 2.

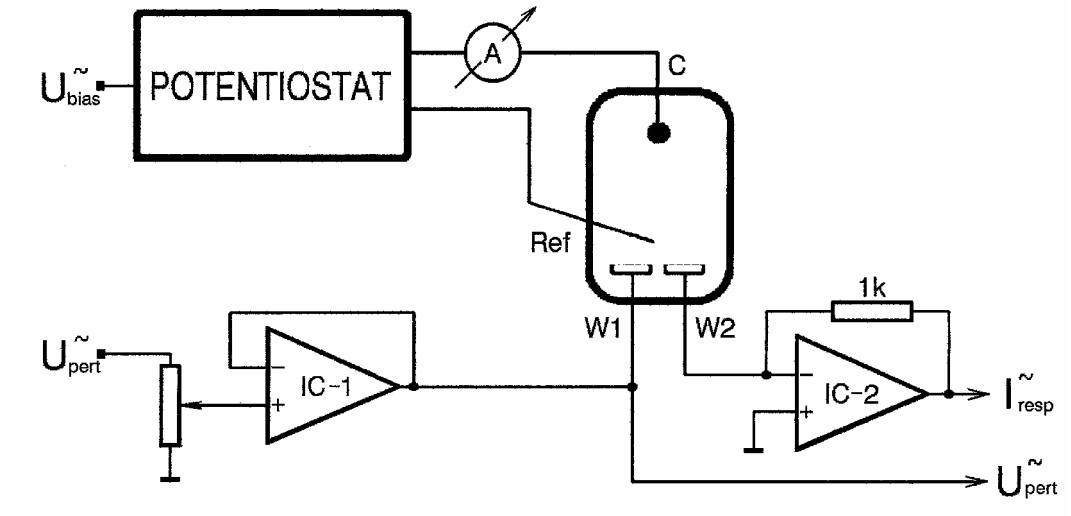

Fig. 2 Electronic circuit diagram of impedance measurement on twin electrode

An equal bias potential U_{bias}, measured against the reference electrode, was applied to both W_1 end W_2 electrodes. Small perturbation voltage $\widetilde{U}_{pert}$ with peak-to-peak amplitude 15 mV was applied to the electrode W1. The perturbation voltage $\widetilde{U}_{pert}$ and the resulting current between W_1 and W_2 was used to calculate the impedance of the twin-electrode at the preset bias electrode potential U_{bias}.

2.2 Cells and Electrodes

2.2.1 Three-electrodes-cell

A multifunctional three electrode cell, presented below, was used for all measurements.

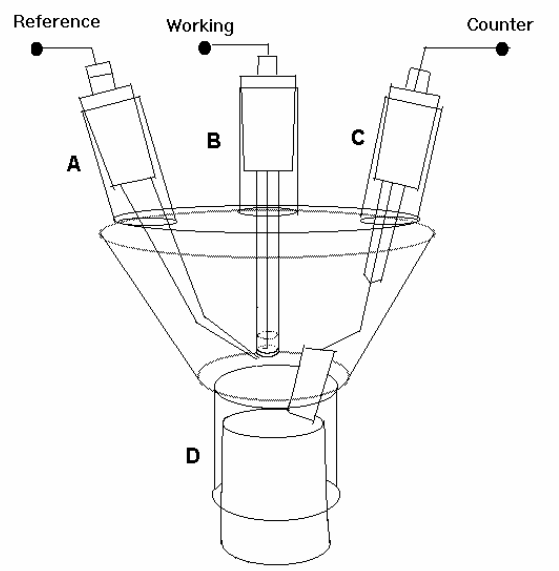

Fig. 3 The multifunctional 3 electrode cell used for electrochemical measurements

It was made out of Jena glass and rid up with 4 ground glass stopper sockets A,B,C and D for attachment of different electrodes. For most of measurements two such cells were used. One was filled with electrolyte, containing monomer and used for preparation of polymer films as well as for investigation of the polymerization process. After the preparation of polymer layer the stopper with the working electrode was removed from the socket B, rinsed in clean acetonitrile for 5 minutes and then placed in the socket B of the second analogous cell, filled with free of monomer electrolyte.

For all measurement a nonaqueous reference electrode was used. As reference, the couple Ag/0.01 M $AgNO_3$ +0.1 M TBAB was chosen. It is reversible and rapid in acetonitrile and has a potential +0.291 V vs. SCE as reported in [*lii*]. The reference electrode was mounted together with a Lugging capillary into a polyethylene stopper, as shown in Fig. 4, at short distance to the working electrode to prevent for possible disturbances.

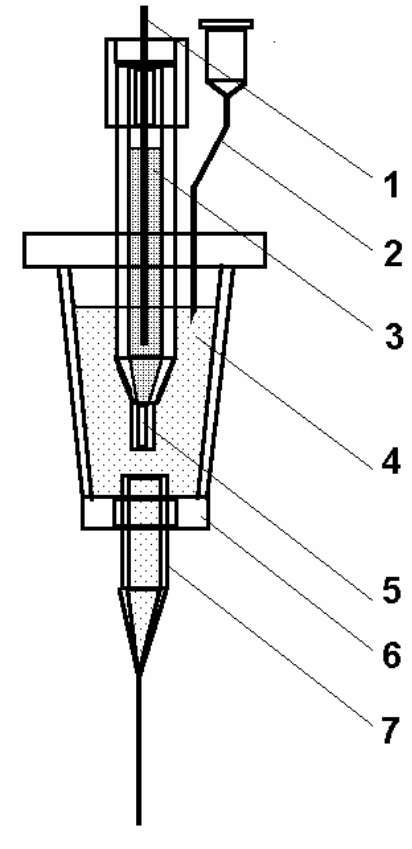

Fig. 4 The reference electrode used for electrochemical measurements in the 3-electrode cell.

1. *Silver wire*
2. *Syringe needle for filling the Luggin capillary tube with the electrolyte*
3. *Ag/0.01M $AgNO_3$ solution in acetonitrile*
4. *Electrolyte solution hoisted from the cell*
5. *Frit membrane*
6. *Polyethylene stopper*
7. *Polyethylene Luggin capillary tube*

A Platinumum wire melted into a glass tube and cut off near the glass range served as the working electrode. The cut was grounded with emery paper. The diameter of the used Platinum wire determined thus the diameter of resulting disc electrode and was chosen specially for every particular experiment. The glass tube with the Platinum wire was fixed in a polyethylene stopper as shown in Fig. 3. Platinumum wire melted in a glass tube and fixed analogously in a polyethylene stopper was used as the counter electrode. All measurements were performed under Ar atmosphere.

2.2.2 The twin electrode

The twin-working electrode used for impedance measurements with one-side contacted polymer layer was constructed analogous to one described in [31]. It possessed a sandwich configuration consisting of two sheets of Pt with an insulation foil in between, pressed together with a very little amount of epoxy seal and stored under pressure till hardening (24 hours). The so prepared „sandwich“ was inserted into a glass stopper and sealed in epoxy resin, high resistive against organic solvents, which was hardened by 120° for 20 minutes. The surface directed to the socket was grounded with series of different emery papers with dimension of abrasive particles from 30 to 0.05 μm. The

two Pt stripes, 5 mm × 0.5 mm each, separated by a 20 μm gap appeared after the preparation as shown below.

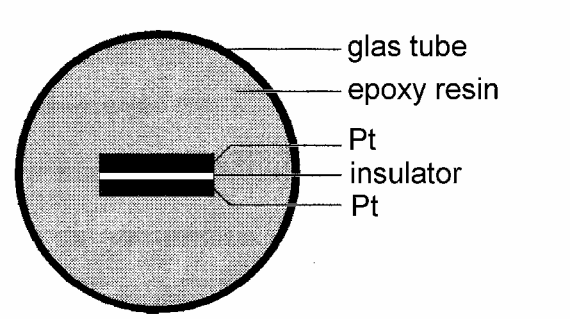

Fig. 5 Cross section of the twin-working electrode. Platinum strips: 5 mm × 0.5 mm each, gap: 20 μm.

The glass stopper with incorporated twin electrode was inserted into the socket D in Fig. 3 and the bands of the twin electrode was then covered with polymer layer by electrochemical polymerization in solution containing monomer. Dependent on the particular experiment it was then rinsed with clean acetonitrile and placed in socked D of an another cell with free from monomer electrolyte for further measurements.

2.3 Chemicals and Electrolytes

The acetonitrile used for preparing of all electrolyte solutions was „acetonitrile extra pure“ from Merck, Art. 15500, which was stored for 30 minutes with heated Na_2SO_4, then distilled from $KMnO_4$, processed with small amount of concentrated H_2SO_4 and then finally distilled from P_2O_5 as described in [*liii*].

TBAB (tetrabutilamoniumborfluorid) was used as the conducting salt. It was supplied by Fluka, cleaned by recrystallization from double distilled water and dried by 80° under vacuum. The background current measured to prove the absence of electroactive species in the electrolyte on Pt electrode at 1.2 V vs. SCE has been found to be 7 $\mu A \cdot cm^{-1}$.

Bithiophene (Merk) was used as supplied, Pyrrole (Merk) was distilled under vacuum in Ar atmosphere and stored in a refrigerator by -5°.

Electrolytes containing 0.05 M of monomer were used for electropolymerization in all experiments.

3 Basic experimental data analysis

3.1 The analysis of the impedance spectra of conducting polymer layers

The EIS spectra of conducting polymers are quite complex and still not well understood because of numerous processes taking place simultaneously during recharge of the polymer layer. However, a number of models, describing the impedance spectra for some particular kind of polymer layers, has been proposed in the literature [6,27,liv,62-66]. In this work only the models, describing the capacitive effects in the low frequency range through chemical processes, as first proposed by Hunter et al.[6], have been applied. This well known from the literature approach emphases the restricted amount of the electroactive species on the interface of the electrode as the reason for the capacitive behavior of the polymer layer in the low frequency region. The mechanism of this kinetical effect can be demonstrated on the example of the simplest representative of such systems - the monomolecular layer of electroactive species fixed on the electrode. The probability of diffusion of the dopping ions from the electrode interface into a polymer layer with a finite thickness [48] and the influence of the porosity of the electroactive layer [27] are the complications solved by two models presented further in this chapter.

3.1.1 Monolayer of an electroactive species

Monomolecular layer of electroactive species, fixed on the interface, is the simplest representative of the electroactive coatings and offers thus a favorable object for illustrating the common properties, shared by more complicated systems. An electrochemical behavior of such a system at higher frequency range is analogous to one, characteristic for species dissolved in the electrolyte. The charge transfer resistance R_{ct} in parallel with the double layer capacitance C_{dl} results in a semi-circle in the impedance spectrum, if presented as a Nuquist plot. The change of the concentration of the electroactive specie during the harmonical perturbation of potential becomes significant at lower frequencies and leads to more complicated impedance behaviour.

To evaluate the quantitative correlation between the kinetic characteristics of this system and its impedance spectrum it can be helpful to make use of the equivalent circuit presented below, known as the Randles circuit.

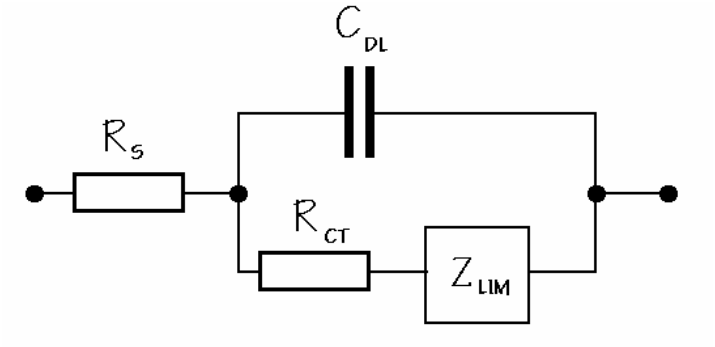

Fig. 6 Randles equivalent circuit for the ac response of an activated charge transfer and concentration hindrance of reaction. R_s is the serial resistance of electrolyte, C_{dl}, the double layer capacity, R_{ct}, the charge transfer resistance and Z_{lim} is the concentration hindrance impedance.

This circuit describes a behavior of all non distributed electrochemical systems, if only one redox couple is present and the Z_{lim} is considered to be any kind of a concentration hindrance, i.g. Warburg impedance for the case of an active specie, dissolved in electrolyte. The evaluation of the impedance of electroactive monolayer, fixed on the electrode is thus simplified to the determination of the expression for $Z_{lim.}$ Evaluation of this impedance means finding the relation between the small perturbation voltage δE, and the response current δi under the assumption, that no charge transfer resistance or double layer capacity is present. In this case the flow of charge δQ is linearly connected with the change of the concentration of the oxidized species by the Faradaic law. Assuming further, that δE/δt = dE/dt, δE/δQ = dE/dQ for small amplitude of perturbation potential, the definition of the current i=δQ/δt can be rearranged, as

$$i = \frac{dE}{dt}\frac{SFz}{dE/dc} \qquad \textit{eqn. 1}$$

Here c is the interfacial concentration of the oxidized species, S, the interface of the electrode, F, the faradaic constant and z, the number of electrons involved in the reaction. This expression is analogous to the equation describing the current response of

capacitor. Hence it is justified to denote the time independent multiplier as „pseudocapacity“, C_{ps}.

$$i = \frac{dE}{dt} C_{ps} \qquad C_{ps} = \frac{SFz}{dE/dc} \qquad \textit{eqn. 2}$$

If the systhem exhibits an ideal behaviour, the dependence dE/dc can be determined by differentiating the Nernst's equation. The corresponding equation for C_{ps} for such a system is then given as:

$$C_{ps} = \frac{F^2 c_0 z}{RT} \frac{\exp\left[\frac{zF}{RT}(E - E_0)\right]}{\left\{\exp\left[\frac{zF}{RT}(E - E_0)\right] + 1\right\}^2} \qquad \textit{eqn. 3}$$

Here c_0 is the sum of interfacial concentrations of the oxidized and reduced species, E is the bias electrode potential, at which the small alternating voltage δE is applied and E_0 is the formal potential of the redox couple. It can be seen, that the observed system exhibits an impedance behavior of a capacitor, which capacitance varies with the bias electrode potential. The peak of the capacitance value is reached at the formal potential of the particular redox couple.

3.1.2 Homogenous nonporous electroactive layers

If thin, but not monomolecular layers of the electroactive substance has to be considered, as normally the case with conducting polymers, a diffusion of dopping ions into the inner parts of the layer has to be taken into account. The analysis of the ac current response of such a system is given by Ho et al. [48]. Analogously to the approach used in chapter 3.1.1, the Randles equivalent circuit can be used. The Z_{lim} has to be evaluated considering the gradient of concentration at the interface, described by the Fick's law. The solution of the Fick's differential equation

$$\frac{\partial[\delta c(x,t)]}{\partial t} = \tilde{D} \frac{\partial^2[\delta c]}{\partial x^2} \qquad \textit{eqn. 4}$$

with the boundary conditions dc(*0,t*)=0 and dc(*l,t*), as given by eqn. 2, allows to determine the impedance of the concentration hindrance as:

$$Z_{rfW} = \frac{dE}{dc}\frac{1}{zF}\frac{\coth(l\sqrt{i\omega/D})}{\sqrt{i\omega D}} \qquad \textit{eqn. 5}$$

Here Z_{rfW} is the "restricted finite Warburg" impedance and *l* is the thickness of the layer. The impedance of the equivalent circuit shown on Fig. 6, with the Z_{rfW} substituting Z_{lim}, is given by:

$$Z_{Ho} = \left[\left(\frac{1}{Z_{rfW} + R_{ct}} + i\omega\, C_{dl}\right)S\right]^{-1} \qquad \textit{eqn. 6}$$

An example of an impedance spectra of such a system is shown as Nuquist plot below.

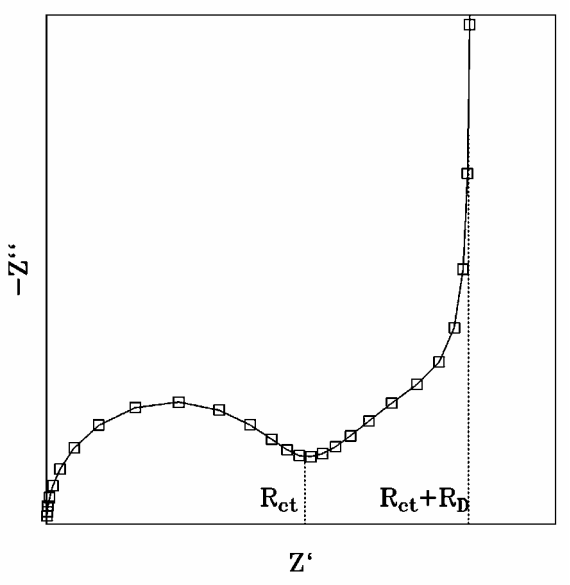

Fig. 7 Computer simulation of the impedance of homogenous nonporous layer of electroactive species using the equivalent circuit shown in Fig. 6 with restricted finite Warburg impedance as concentration hindrance.

It can be seen, that the kinetics changes from charge transfer control by high frequencies to diffusion control by intermediate frequencies. At very low frequencies range, the effect of the finite layer thickness becomes dominant and the restricted finite Warburg impedance approaches the impedance of a capacitor C_{ps}, connected in series with a resistance $R_{D.}$ The values of this elements can be expressed as:

$$C_{ps} = l\frac{SFz}{dE/dc} \qquad R_D = l\frac{dE/dc}{3DSFz} \qquad \textit{eqn. 7}$$

It can be seen, that the pseudocapacity for the case of a multimolecular layer is expressed analogously to one of the monomolecular layer with the difference, that here c is the volume concentration of the electroactive species. dE/dc can be determined by differentiating of the Nernst's equation (cf. eqn. 3), if the particular redox couple exhibits ideal behavior.

3.1.3 Porous electroactive layers

Thick polymer layers exhibit impedance behavior, which can not be described by the simple model, presented in the previous chapter. The semicircles observed in the higher frequency range in the complex impedance plots are depressed, which can be accounted for the distribution of the time constants. The possible reason for such a distribution for the case of conducting polymer layers could be their high porosity. Paasch et al. [27] have proposed a theoretical model, which allows an analysis of systems exhibiting such behavior. In this theory the polymer layer is assumed to be a macrohomogenous two-phase system consisting of small polymer aggregates and electrolyte. The diffusion of the dopping ions occurs inside of this aggregates, therefore the characteristic diffusion length can be assumed to be independent of the polymer thickness, corresponding to results of experimental measurements of Tanguy et al. [9]. To find the total impedance of such a system, the entire polymer layer is divided into N elementary volume elements with cross-sections A. The polymer is assumed to be contacted to polymer and the electrolyte to electrolyte at each cross-section.

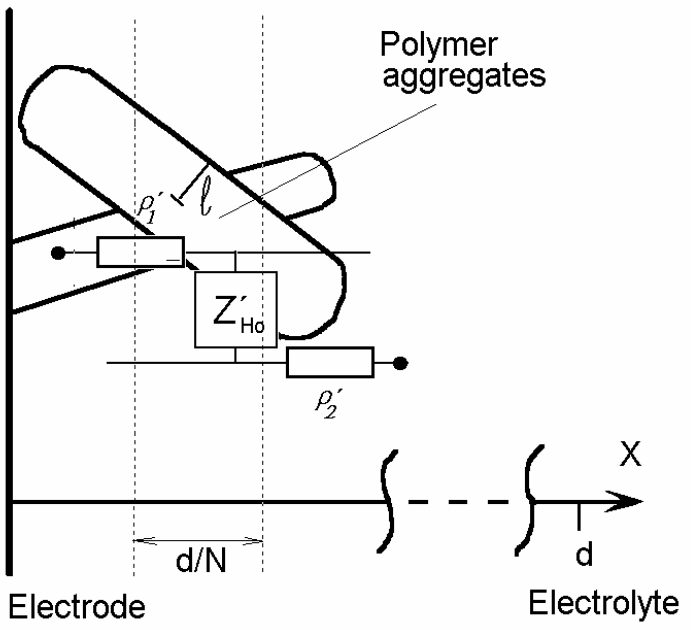

Fig. 8 An elementary volume of the porous polymer layer and the corresponding equivalent circuit as assumed by model of Paasch et al.

The charge transfer through the polymer-electrolyte boundary at each cross-section is determined as in the model of Ho et al. under consideration, that the diffusion of the dopping ions take place inside of the elementary agglomerates of the polymer, having a characteristic dimension l, and not through the whole polymer layer. This interfacial impedance can therefore be expressed as

$$Z'_{Ho} = \left[\left(\frac{1}{Z^*_{rfW} + R_{ct}} + i\omega C_{dl} \right) \cdot \frac{Sf}{d} \right]^{-1} \qquad \textit{eqn. 8}$$

The effective interface of the polymer agglomerates inside one elementary volume is given here by the expression Sf/d, where f is the effective interface coefficient and d the thickness of the polymer layer. The Z_{rfW} is calculated analogously to eqn. 5 with the difference, that the diffusion length *l* is treated as the average dimension of polymer aggregates independent on the layer thickness. The current flow through each cross-section is determined by an electronic resistance of the polymer ρ_1, interfacial impedance Z'_{Ho} and the ionic resistance of the electrolyte ρ_2. The impedance the entire

polymer layer is then analogous to one of a transmission line consisting of chain connected elements shown in Fig. 8.

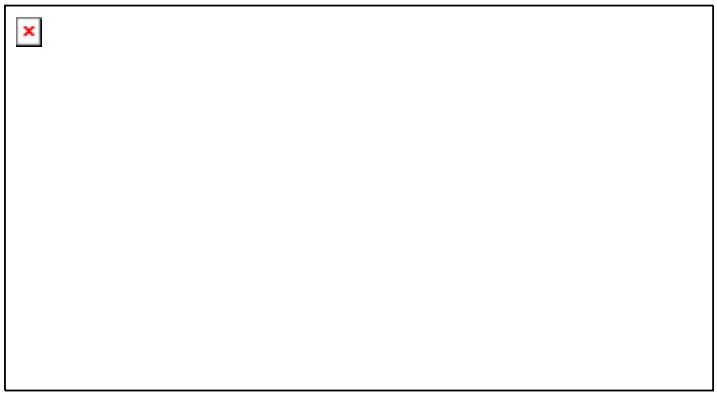

Fig. 9 Generalized transmission line representing the impedance of porous macrohomogenous electrode

The solution for the input impedance of this circuit under consideration of infinite N is given by Paasch et al. However, for the case of oxidized or slightly reduced conducting polymers, the expression for the total impedance of presented generalized transmission line can be considerable simplificated by an assumption, that either electronic or ionic resistance of the polymer layer is neglectable small. The impedance of a cross-connected transmission line will then be equal to the impedance of normal transmission line, terminated by an impedance Z_t.

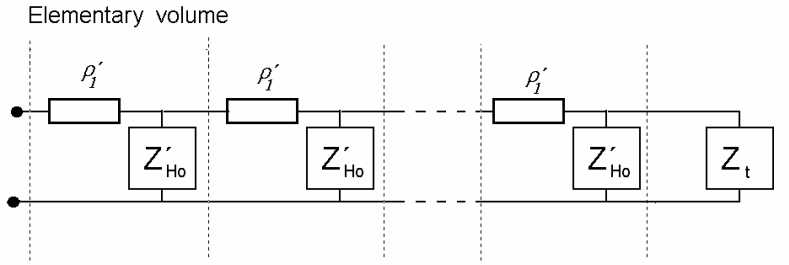

Fig. 10 Generalized transmission line representing the impedance of porous macrohomogenous electrode neglecting the specific resistance of the polymer or of the electrolyte.

The terminating impedance Z_t can be either infinity for a normal impedance measurement or zero for measurement on polymer layers contacted only on the electrolyte side or on the polymer side. The expression for the total impedance of this

circuit under consideration of an infinite small distance δx and Z_t equal to infinity is derived by Fletcher [*liv*]:

$$Z = \sqrt{Z_{Ho}\,\rho/S}\cdot\coth\left(d\cdot\sqrt{\frac{\rho/S}{Z_{Ho}}}\right)+R_s \qquad \textit{eqn. 9}$$

The serial distributed resistance per unit length ρ'_1 is replaced here by ρ/S, where ρ is the specific resistance of the polymer. A computer simulation results for the same parameter using eqn. 6 and eqn. 9 are presented below.

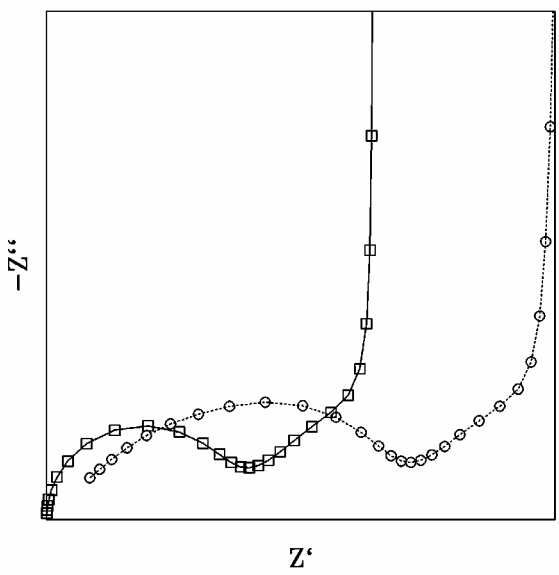

Fig. 11 Computer simulation of impedance spectra for the same parameters using Ho et al. model (eqn. 6)- solid line, and simplified Paasch et al. model (eqn. 9)- dashed line. Specific resistance ρ = 4.8 E+5 Ωcm was used in eqn. 9.

In the low frequency region the impedance spectra predicted by the model is practically analogous to one of serial connected resistance R and capacity C. The interpretation of this quantities is similar to one given in eqn. 7. The difference is in the additional serial resistance R_l, which accounts for the resistance of polymer and is related to the specific resistance as

$$R_l = \rho d/3S \qquad \textit{eqn. 10}$$

3.2 Field considerations for measurements on the twin electrode

The specific conductivity of an electrochemically deposited polymer layer is an essential electrochemical characteristic. However, the conventional impedance measurements, where the polymer layer is contacted on both polymer and electrolyte sides, do not allow to distinguish between the electronic conductivity of polymer itself and the ionic conductivity of the electrolyte in pores. Conductivity measurements between the bands of a twin-electrode, as shown in the picture below, covered with a polymer layer, was proposed by several authors for this purpose [11,12,29].

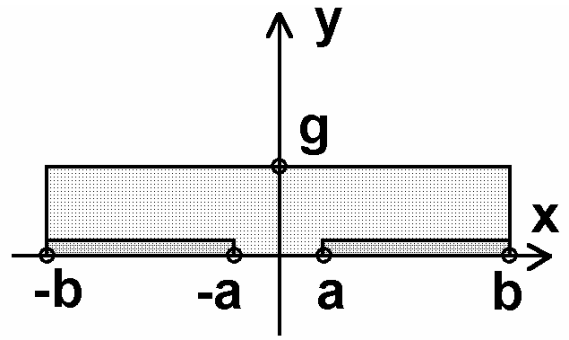

Fig. 12 Cross-section of a twin electrode covered with a polymer layer of thickness g.

The polymer-electrolyte interface, which is partly present also inside of the polymer layer because of its porosity, has highly capacitive character. Therefore, high frequency ac current flows between the electrodes not only trough the polymer but can also across the walls of cavities and uses the electrolyte as an alternating path. This effect is diminished by very low frequencies, however, where the pure electronic resistance can be measured.

Measurements between the bands of the twin-electrode can be applied to obtain the value of conductance, which can be used to compare polymer layers with different oxidation level, but depends on the particular electrode configuration. To evaluate the specific conductance of polymer layer, an analysis of electrical field between the bands of the twin electrode is required.

The theory of conformal mapping was applied by Kankare et al. [29] to find the solution of the current flow field for the electrode configuration analogous to this used in our work. According to this approach, the electrode configuration depicted into complex

coordinate plane is transformed with preserving the angles between the boundaries into another complex plane, where the solution of the field can be easily found. For the transformation of the polygonal boundaries, the Schwarz-Christoffel equation is usually used to calculate the transformation function of the coordinates. The authors have shown, that the configuration in Fig. 12 can be transformed to a plate-capacitor-like configuration:

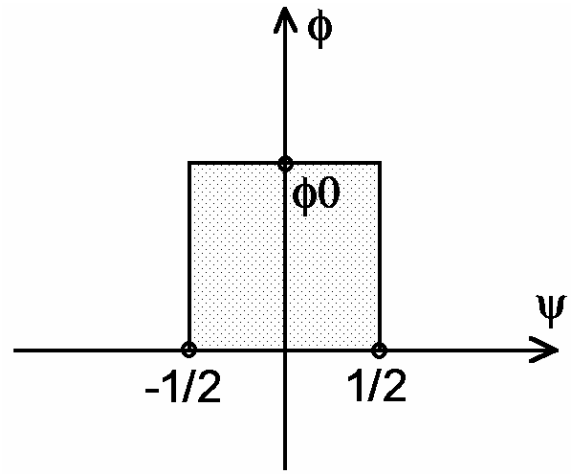

Fig. 13 Space obtaining by two-stage conformal mapping of the configuration shown in Fig. 12 with the polymer layer mapped into the interior of a rectangle and electrodes into the opposite sides of the rectangle.

The virtual width of the electrodes, $\phi 0$, in this new complex coordinate system can be expressed through the coordinates of electrodes in the original plane as [*lv*]

eqn. 11

$$\phi 0 = \frac{K'(k)}{2K(k)} \qquad k = \frac{\tanh(\frac{1}{2}\pi\frac{a}{g})}{\tanh(\frac{1}{2}\pi\frac{b}{g})}$$

Here, a and b are dimensions of the twin-electrode and g the thickness of the layer, as in Fig. 12; K(k) and K'(k) are complete elliptic integrals modulus k of first and second kind respectively, as in

$$K(k) = \int_0^1 \frac{1}{\sqrt{(1-x^2)(1-k^2x^2)}}dx \qquad K'(k) = \int_1^{\frac{1}{k}} \frac{1}{i\sqrt{(1-x^2)\left(1-k^2x^2\right)}}dx$$

eqn. 12

The configuration shown in Fig. 13 is one of a plate capacitor thus the conductance between the two plates is given by:

$$G = \sigma l \phi 0 \qquad \textit{eqn. 15}$$

Kankare et al have shown, that the expression for conductance G can be simplified for the case of an intermediate layer thickness (a < g < b) as in eqn. 13.

$$G \approx \frac{\sigma l}{\pi}\left(\ln\frac{8}{\pi a} + \ln g\right) \qquad \textit{eqn. 13}$$

In the region g > b the resistance between the bands of twin electrode becomes independent on the of the layer thickness:

$$G \approx \frac{\sigma l}{\pi}\ln(4b/a) \qquad \textit{eqn. 14}$$

Using these two expressions, thickness and specific resistance of the polymer layer can be determined, if the dependence of conductivity between the bands of the twin electrode on polymerization charge is known. Assuming, that the thickness of deposited polymer layer depends linearly on the charge used for polymerization per unit area (g = kQ) , eqn. 13 can be rearranged as follows:

$$G \approx \frac{\sigma l}{\pi}\left(\ln\frac{8k}{\pi a} + \ln Q\right) \qquad \textit{eqn. 16}$$

Accordingly, the specific conductivity can be calculated from the slope of G vs ln Q. The intercept gives the thickness growth coefficient k.

$$\sigma = \frac{\pi}{l}\tan(\alpha) \qquad k = \frac{\pi a}{8}\exp(G(0)\pi/\sigma l) \qquad \textit{eqn. 17}$$

An example of a dependence of G on Q, simulated for a dummy twin electrode is shown in Fig. 14.

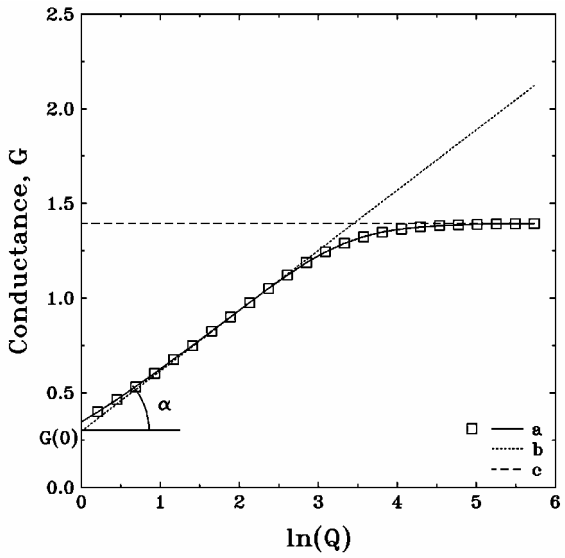

Fig. 14 Conductance between the bands of the twin-electrode vs. ln(Q) exact simulated using eqn. 15 (a) and approximately simulated using eqn. 13 (b) and eqn. 14 (c). Here, a=1, b=20 and l=k=σ=1 were used in simulation.

3.3 Complex nonlinear least squares fitting

EIS spectra are often complex and can give only qualitative information about properties of the examined electrochemical system. Quantitative informations can be obtained by fit of experimental data to a complex function resulting from the used physical model. For this purpose, the complex nonlinear least squares (CNLS) immittance fitting program LEVM 6.1 by J.R.Macdonald [*lvi*] was used and modificated in this work.

The least squares fitting procedure optimizes parameters of the used physical model by minimizing the sum:

$$S(P) = \sum_j w_j \left[Z_j - Z(\omega_j, P)_j \right]^2 \qquad \textit{eqn. 18}$$

Here, Z is the vector of experimental impedance values for each frequency, Z(P) is the functional dependence of impedance on frequency **ω** and vector of parameters P, resulting from a particular physical model. The sum is calculated in range j = 1-N, where N is the total number of experimental data points. W is the vector of weights for each point. Weighting factor w_j is calculated from the uncertainty of the jth data point, β_j, as follows:

$$w_j = 1 \Big/ \left(\beta_j \right)^2 \qquad \textit{eqn. 19}$$

Levenberg-Marquardt algorithm [*lvii*] is used to minimize the sum in eqn. 18. Relative and absolute standard deviations for each parameter fitted are calculated during the minimization. These values were used to check the goodness of the entire fit as well as to reveal the effect of any parameter on the function value in view of a particular parameter set. The value of relative deviation for every parameter is conversely proportional to its average partial derivative over the frequency range where the fit is performed. The parameters having insignificant effect on the functional value in considered frequency range would therefore be calculated with very large relative deviations. This makes the error variance analysis important for validation of the parameter reliability.

4 Results

4.1 Impedance measurements during oxidation and reduction of conducting polymers

4.1.1 Simulation procedure

As well known from measurements performed under potential control, the low frequency impedance of polymer covered electrodes can be approximated by a capacitance and a series resistance [6,lviii-lx]. The nature of the capacitance is still not well understood. It is often referred to as "limiting", that reflects its connection to the finite diffusion at limiting low frequencies, or as "redox" to point out its relation to oxidation/reduction processes of the polymer film.

In order to simulate the capacitive part of the current-voltage curve we assumed that the equivalent circuit of the cell can be represented as a series combination of a resistor R and a capacitor C, both dependent on the applied electrode potential U. Then the potential drop U_c across the capacitor when current I flows is

$$U_c = U - IR \qquad \textit{eqn. 20}$$

and the charge $Q = U_c \cdot C$, stored in the capacitor is

$$Q = (U - IR)C \qquad \textit{eqn. 21}$$

Taking into account the dependence of R and C on the potential and assuming a constant sweep rate $\upsilon = dU/dt$ in cyclic voltammetry, differentiation of eqn. 21 gives

$$\frac{dQ}{dt} = \left[\upsilon - I\upsilon\frac{dR}{dU} - R\frac{dI}{dt}\right]C + \upsilon(U - IR)\frac{dC}{dU} \qquad \textit{eqn. 22}$$

which can be rearranged to give the differential equation for the current as

$$\frac{dI}{dU} + \left[\frac{1}{\upsilon RC} + \frac{1}{R}\frac{dR}{dU} + \frac{1}{C}\frac{dC}{dU}\right]I = \frac{1}{R} + \frac{U}{RC}\frac{dC}{dU} \qquad \textit{eqn. 23}$$

The solution of eqn. 23 for I = I(U) has been obtained numerically using the Runge - Kutta method. The data for R(U) and C(U) used in the calculations have been obtained

from low frequency part of EIS measurements. The anodic and the cathodic sweeps have been simulated separately with the initial conditions $I_{+,start} = 0$ at the start of the anodic sweep and $I_{-,start} = I_{+,end}$, where $I_{-,start}$ is the current at the start of the cathodic sweep and $I_{+,end}$ is the current at the end of the anodic sweep. For the sake of comparison, simulation of cyclic voltammograms (CVs) using obtained C(U) data has been also performed using

$$I_c = C(U)\upsilon, \qquad \textit{eqn. 24}$$

neglecting the potential dependencies of C and R, as previously reported by Tangui at al. [9].

4.1.2 Measurements and simulation results

The measurements have been performed on a polished polycrystalline Pt electrode (0.02 cm^2) coated with PBt or PPy layers, obtained galvanostatycally at 2 $mA \cdot cm^{-2}$ for 40 s. The impedance spectra measured during anodic and cathodic potential sweeps at a scan rate of 20 $mV \cdot s^{-1}$ in the ranges - 0.3 to 1.0 V for PBt and 0.4 to 0.7 V for PPy are shown in Fig. 15 and Fig. 16 respectively.

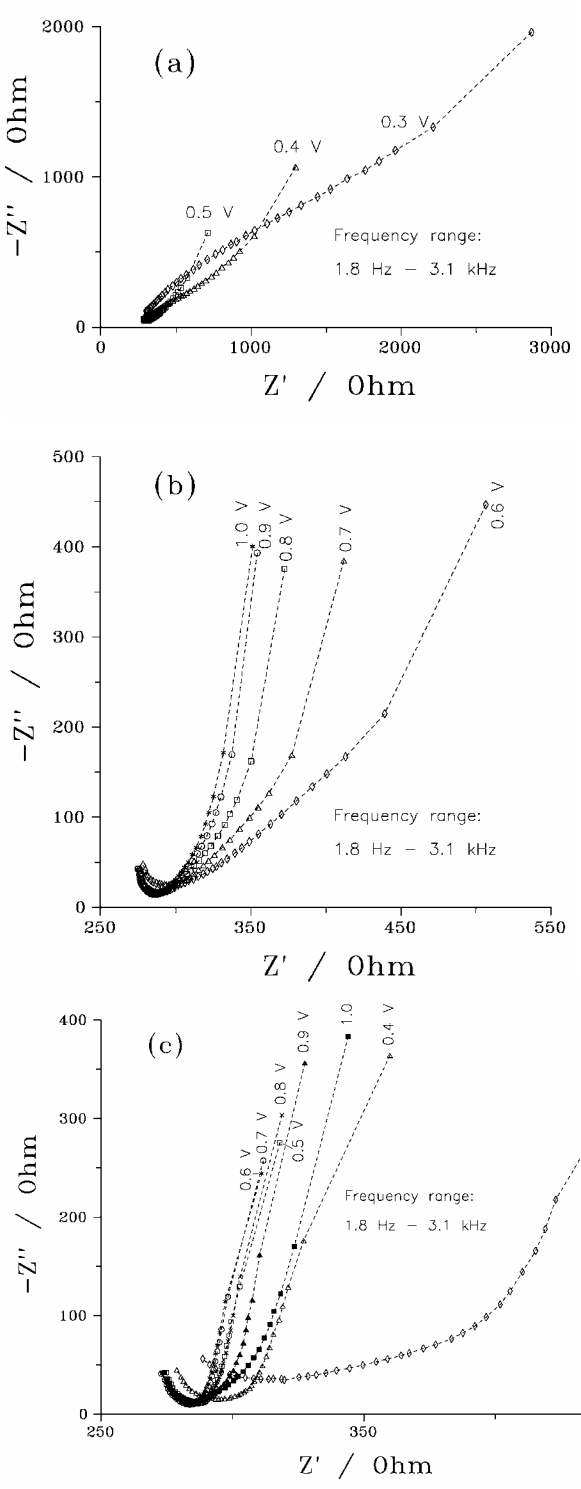

Fig. 15 Complex plane impedance plots for a PBt-coated electrode measured at different electrode potentials: (a),(b) anodic sweep;(c)-cathodic sweep.

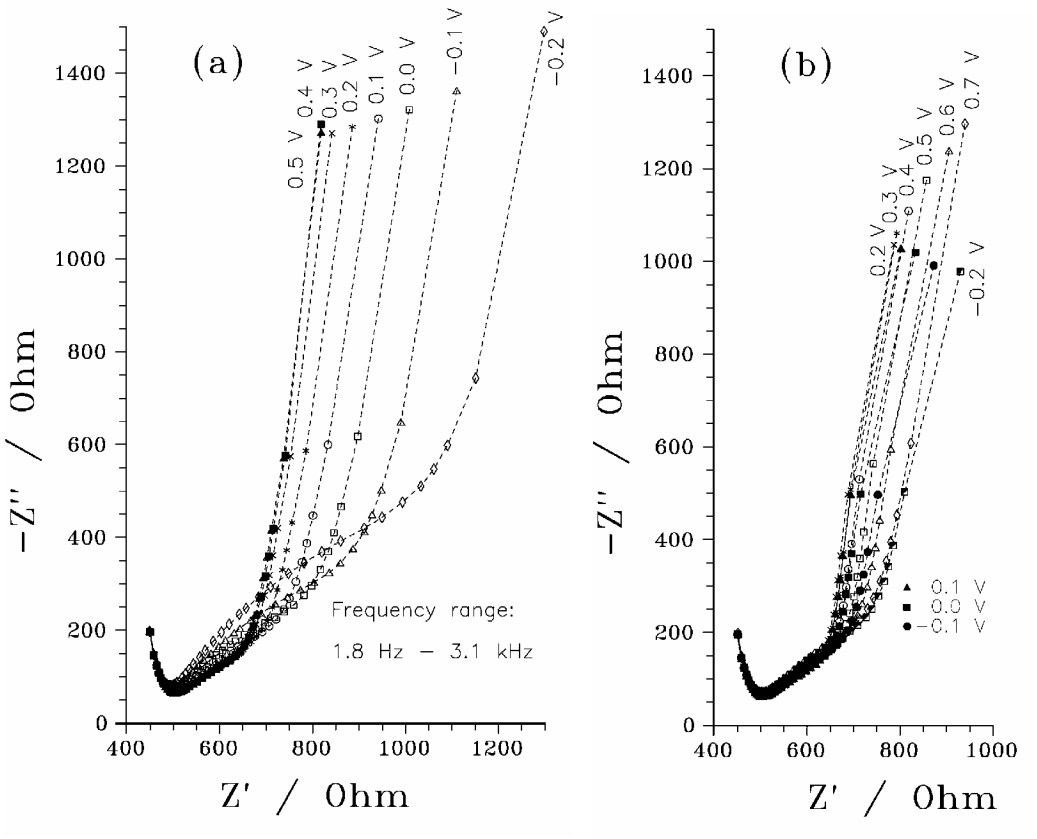

Fig. 16 Complex plane impedance plots for a PPy-coated electrode measured at different electrode potentials; (a) - anodic sweep; (b) cathodic sweep.

It was previously observed, that condition of stady state in polymer layer is reached much faster at potentials, where the polymer is oxidized, then at reducting potentials. Thus, in order to reach reproducible initial conditions for carrying out CV and EIS measurements, the voltammetric cycles were started with the cathodic potential sweep. The potential limits were chosen such that (i) the polymer layer was still slightly oxidized at the end of reduction scan and (ii) high anodic potentials were avoided to prevent the layer from damage due to over-oxidation. The potential dependencies R(U) and C(U) of the resistance and capacitance of the samples, derived from the low frequency parts of the measured impedance spectra, are shown in Fig. 17 and Fig. 18 for PBt and PPy respectively.

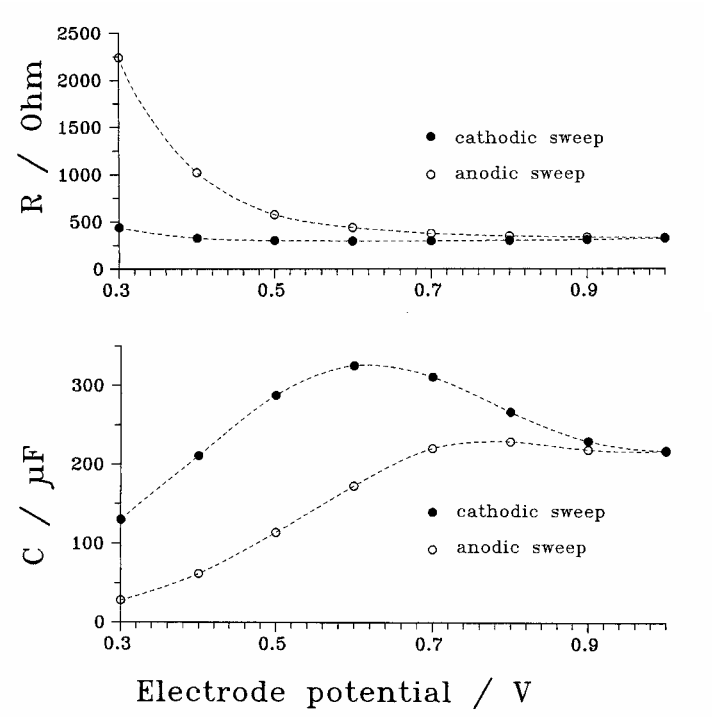

Fig. 17 Capacitance C and resistance R derived for the PBT-coated electrode from impedance spectra measurements.

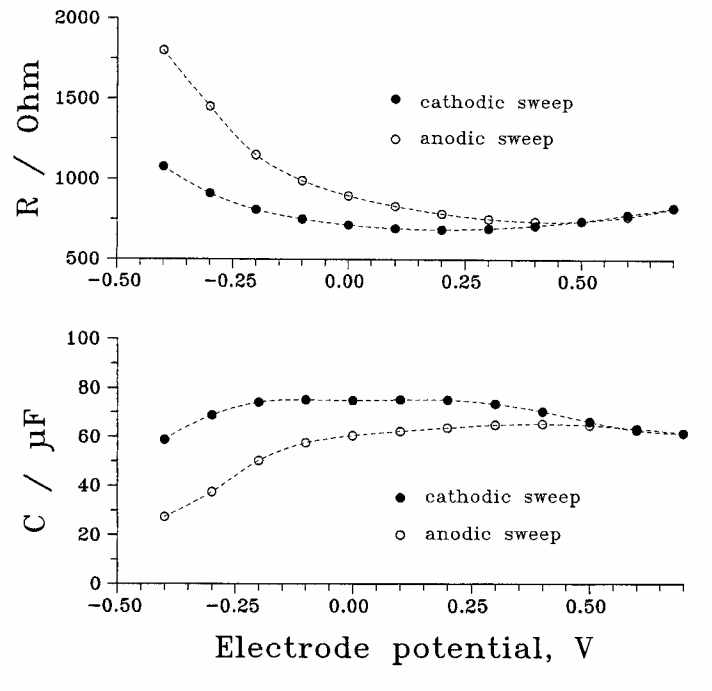

Fig. 18 Capacitance C and resistance R derived for the PPy-coated electrode from impedance spectra measurements.

Results from numerical integration of eqn. 23 and eqn. 24 for the case of PBt are shown in Fig. 19 for the anodic and the cathodic sweeps.

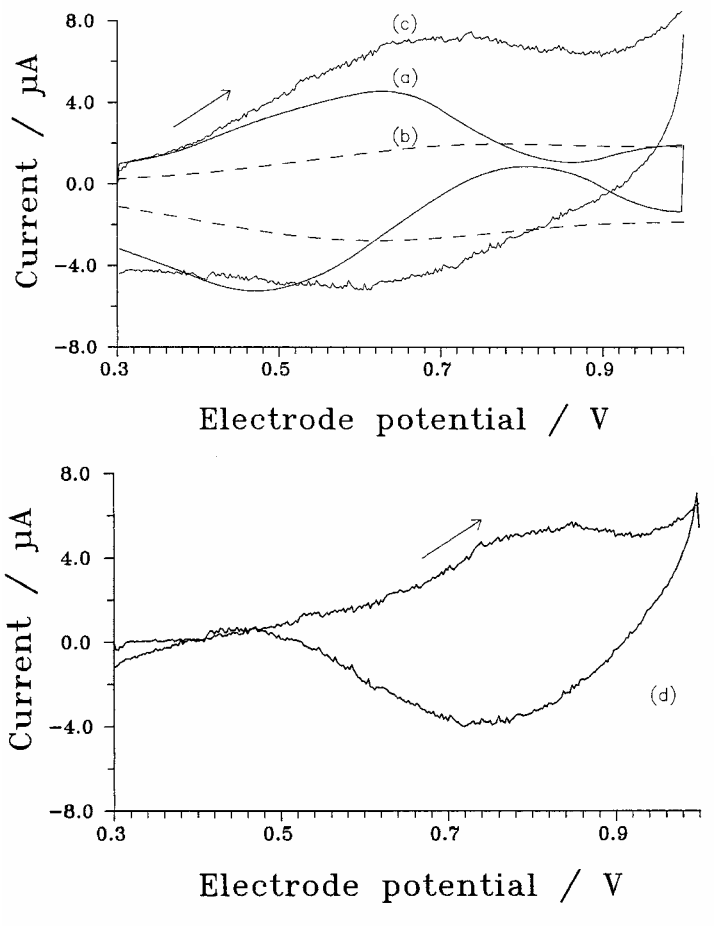

Fig. 19 CV of the PBt-coated electrode. The capacitive current was obtained by numerical integration of (a) eqn. 23 and (b) eqn. 24. The CV recorded experimentally at a scan rate of 8.5 mV· s^{-1} is shown for comparison as curve (c). Curve (d) is the difference between curves (c) and (a).

As mentioned above, the C and R data were derived from a measurement in which the nominal potential sweep rate was 20 mV· s^{-1}. However, the potential sweep was interrupted during the perturbation and data transmission to the computer, so that the effective scan rate was 8.5 mV· s^{-1}. This value was used in the integration and thus a CV recorded at 8.5 mV· s^{-1} is presented for comparison, in Fig. 18. The calculated capacitive current and the measured current-voltage curve for the PPy- covered electrode are shown in Fig 20.

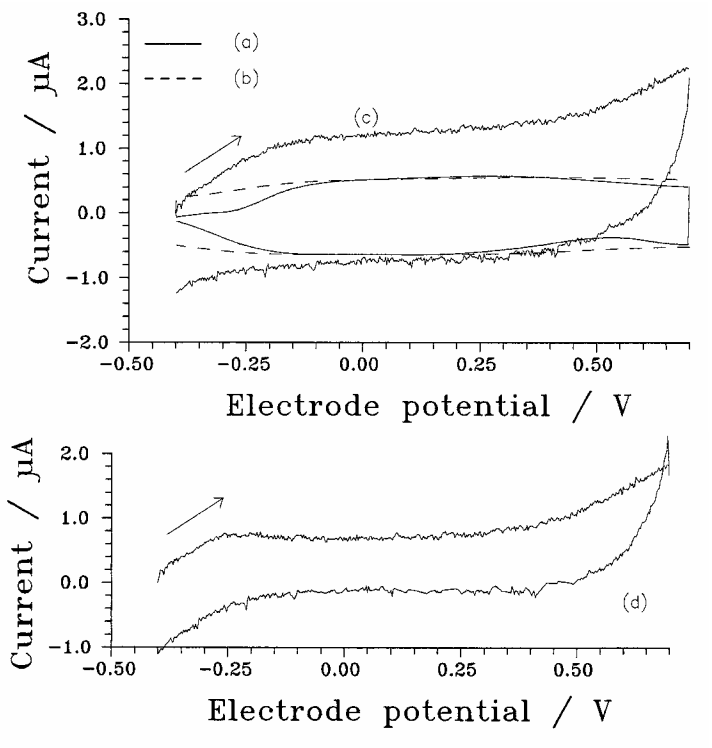

Fig 20 CV of the PPy-coated electrode. The capacitive current was obtained by numerical integration of (a) eqn. 23 and (b) eqn. 24. The CV recorded experimentally at a scan rate of 8.5 $mV \cdot s^{-1}$ is shown for comparison as curve (c). Curve (d) is the difference between curves (c) and (a).

4.2 Impedance measurements on twin working electrodes bridged with polybithiophene layers

4.2.1 Verification of the measurement set-up

As shown in 2.1.3, an application of a perturbation voltage $\widetilde{U}_{pert}$ accross the bands of the twin electrode results in a flow of response current $\widetilde{I}_{resp}$, which can be measured and used for calculating the impedance spectra of the part of the polymer layer, bridging the gap. However, it must be established that the obtained impedance spectra characterize only the polymer layer between the two metal stripes, i.e., that the ac response current, $\widetilde{I}_{resp}$, has no components due to currents crossing the polymer/electrolyte interface.

The twin-working electrode, with the gap bridged by conducting polymer can be represented by a simplified equivalent circuit as depicted in Fig. 21.

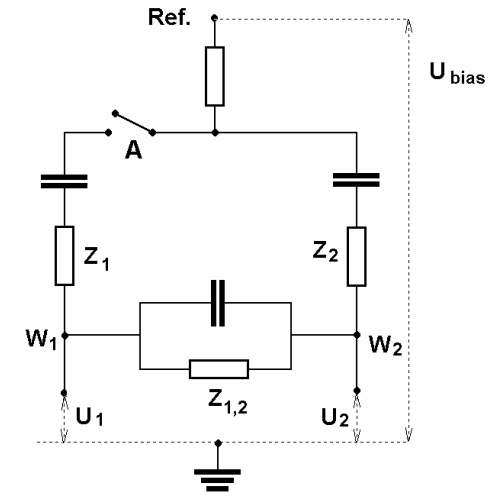

Fig. 21 Simplified equivalent circuit of a twin-working electrode, covered with conducting polymer.

The impedance elements Z_1 and Z_2 represent the metal/polymer/electrolyte branches for the two twin working electrodes, and $Z_{1,2}$ is used for the metal/polymer/metal branch, i.e. for the polymer layer bridging the gap. Note that U_1 and U_2 are given with respect to system ground. When a small perturbation voltage, $\widetilde{U}_{pert}$, is applied to W_1, two currents, $\widetilde{I}_1$ and $\widetilde{I}_{1,2}$, flow through Z_1 and $Z_{1,2}$, respectively. The response current, $\widetilde{I}_{resp}$, measured at W_2 should be equal to the sum of $\widetilde{I}_{1,2}$ and $\widetilde{I}_2$, where $\widetilde{I}_2$ is the a.c. current through Z_2, due to the perturbation. One can consider $\widetilde{I}_2$ as this part of the response current that crosses the interface polymer/electrolyte at W_1, passes through the electrolyte and enters W_2 crossing again the polymer/electrolyte interface. On the other hand the bias voltage, U_{bias}, used to adjust the working potential in an EIS experiment is generally set to be a d.c. voltage, and the fast potentiostat used provides that the potential difference measured between the reference electrode and the working electrode is exactly equal to the preset bias voltage. The working electrode W_2 is connected to virtual ground and it appears as a true working electrode to the potentiostat. Thus, the current across Z_2 depends only on U_{bias}, and does not depend on $\widetilde{U}_{pert}$, i.e. its a.c. component $\widetilde{I}_2 = 0$, and consequently $\widetilde{I}_{resp} = \widetilde{I}_{1,2}$.

Nevertheless, an experiment has been curried out to additionally assure the prevention of cross-interface currents by the measurement set-up. The EIS spectra, resulting from the test measurements, are shown in the figure below:

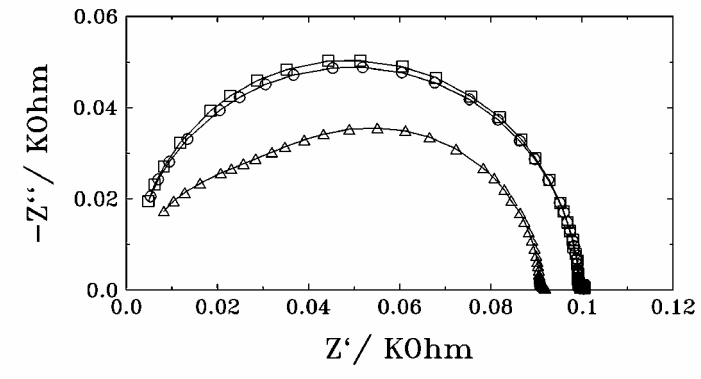

Fig. 22 Impedance spectra measured on the dummy cell shown on Fig. 21. The curve (a) marked with squares - switch A OFF, potentiostat OFF. Curve (b) marked with

triangles- switch A ON, potentiostat OFF. Curve (c) marked with circles- measurement with switch A in position ON, potentiostat control ON.

Curve (a) present a measurement made with a circuit representing interfacial impedance switched OFF. This provide an ideal case, where EIS of the circuit modeling the "metal-polymer-metal" bridge is measured only. In case (b), the normal two-electrode impedance between W_1 and W_2 is measured. Potentiostat is switched OFF, therefore no compensation of cross-interface currents is performed. The impedance spectra corresponds to the electrical circuit W_1-A-W_2 and differ from (a). A reliable measurement of the impedance of the polymer bridge over the gap between the bands of twin electrode is not possible in this configuration. Case (c) occurs in experiments made in a real electrochemical cell. The circuit representing interfacial impedance is switched to ON but the cross-interface current is compensated by the potentiostat, which establishes a constant potential between the pair of working electrodes and the reference electrode. It can be seen, that curves (a) and (c) are almost identical. Thus, the performed test measurements prove experimentally, that the used measurement setup effectively prevents flowing of cross-interface currents.

4.2.2 Impedance spectra

As shown in the previous section, in situ EIS measurements, free of distortion due to current flow through electrolyte, can be performed on twin electrode bridged with polymer layer and can give information about the electrochemical properties of the polymer. Impedance measurements on polymer layers in different oxidation levels were carried out.

The twin-electrode was covered by polybithiophene layer by means of potentiostatical electropolymerization at 0.8 V in monomer solution until the total charge of 800 $mC \cdot cm^{-2}$ passed. The obtained twin-electrode, covered with polymer, was rinsed with acetonitrile and transferred into an electrochemical cell with solution free of monomer. By means of potential sweeps in range 0.3 V - 0.8 V the polymer layer could be reduced and oxidized reversibly. The impedance spectra resulting from the series of EIS measurements, performed for electrode potentials ranging from 0.36 V to 0.8 V are shown in a complex plane diagram.

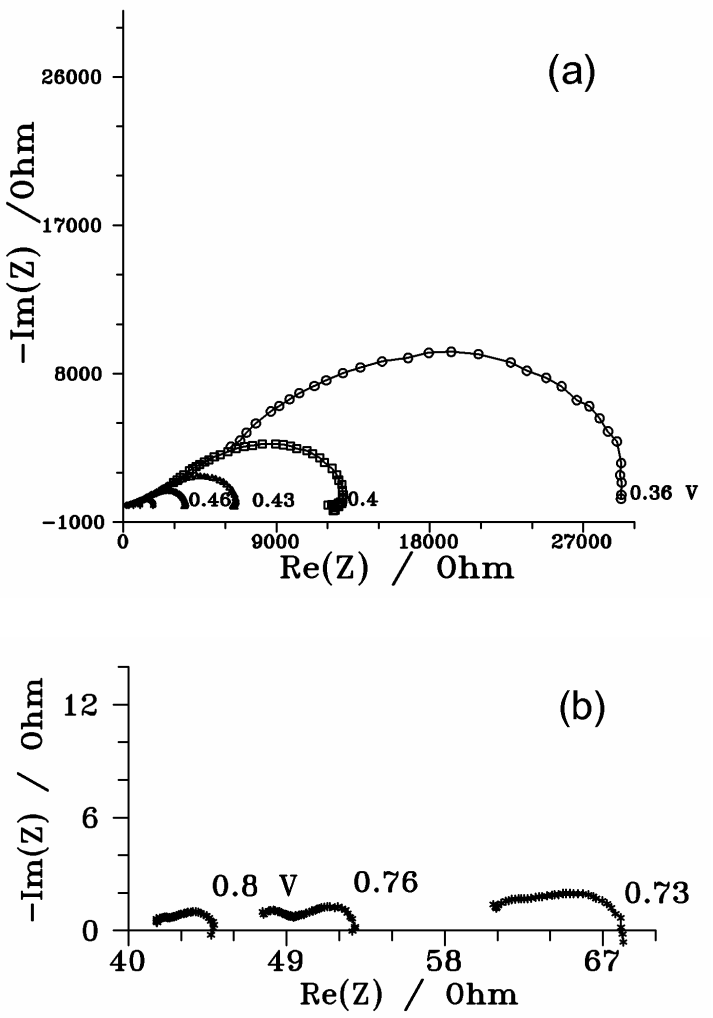

Fig. 23 Series of impedance spectra in the complex plane as obtained during anodic sweep in monomer-free solution in potential range from 0.36 to 0.6 V (a) and from 0.73 to 0.8 V (b).

The results can also be presented as Bode-plots, which allow better comparison of the spectra measured for high and low potentials.

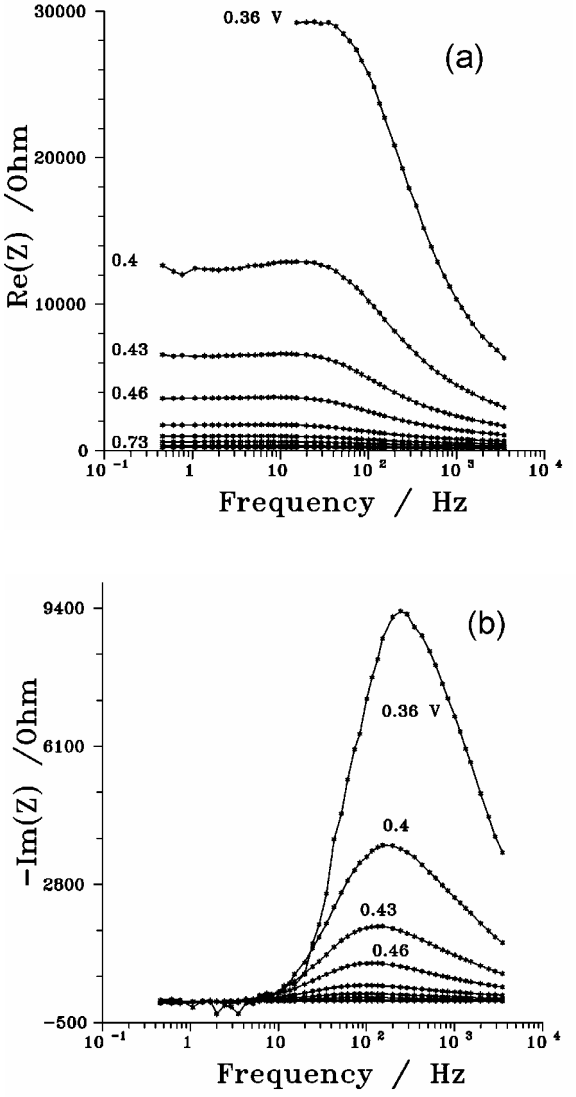

Fig. 24 Series of impedance spectra measured on a polybithiophene covered twin-working electrode during anodic sweep in potential range from 0.36 to 0.8 V presented as Bode-plots.

The values of the resistance between the bands of the twin electrode, extrapolated from the low frequency region of impedance spectra, are presented versus the applied electrode potential:

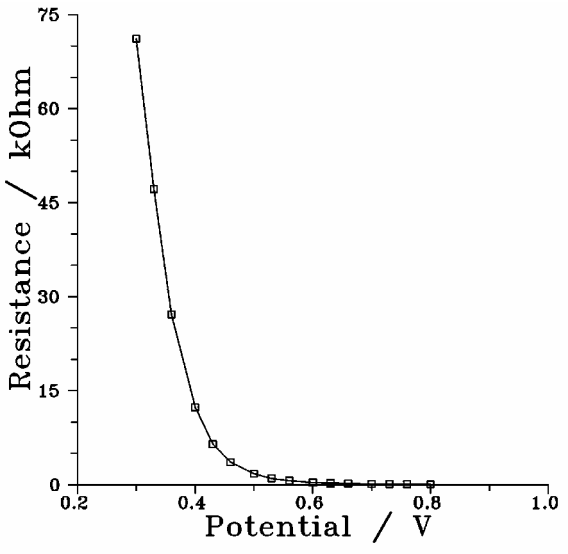

Fig. 25 Resistance data, obtained from the impedance spectra (Fig. 24), measured between the bands of the twin-electrode covered with polybithiophene layers at different electrode potentials.

For the sake of comparison, the two twin- working electrodes were externally short circuited and an impedance spectrum of the polymer-electrolyte interface was measured using the conventional three-electrode cell configuration. Fig. 26 shows the impedance spectrum, as obtained with anodic polarization of 0.8 V, i.e., with the polymer in its oxidized state.

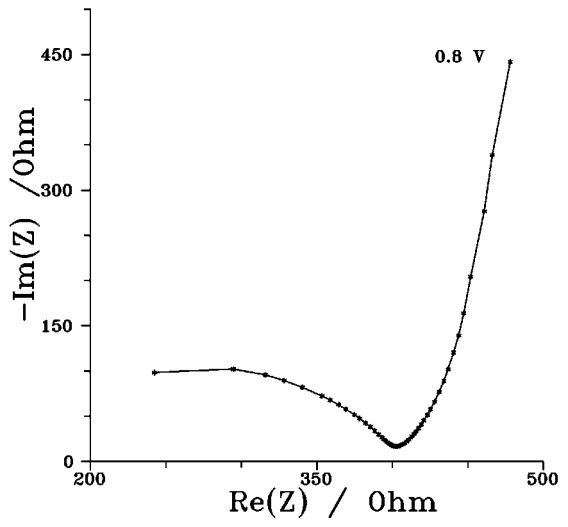

Fig. 26 Impedance spectrum of the twin-electrode, covered with polybithiophene, measured at 0.8 V with a conventional EIS technique with the bands of the twin-electrode connected externally.

As shown in Chapter 3.2, the specific conductivity of polymer layer, deposited on the twin electrode, can be determined by analyzing the dependence of the conductivity between the bands of twin electrode on the charge used for polymerization. The required conductivity data can be obtained from the low frequency parts of impedance spectra, measured between the bands. Aiming to evaluate the conductivity/polymerization charge dependence for a wide range of thicknesses, a series of impedance measurements during a deposition of polymer layer was performed. With this purpose a polished twin-working electrode was subjected to an anodic potential of 0.8 V in a bithiophene solution. The metal stripes were covered with polymer and the growing polymer layer bridged the gap. The charge, Q, passed through the twin-electrode was measured simultaneously by a current integrator and is presented in the figure below.

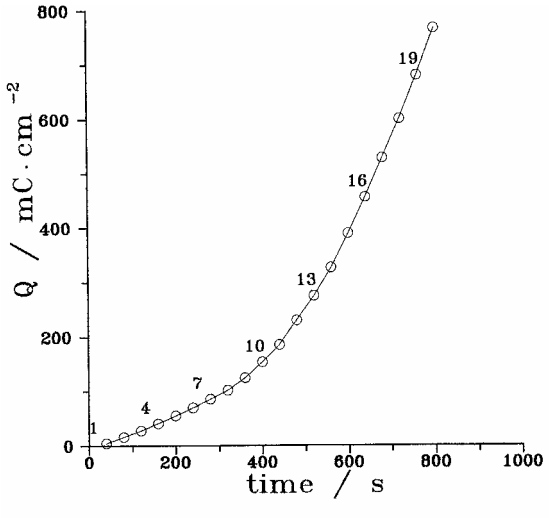

Fig. 27 Total charge, Q, passed through the cell during polymer deposition on the two bands of the twin-electrode. EIS measurements were performed at 40 s intervals as marked with the numbered points.

A series of 20 EIS measurements was performed at time intervals of 40 s after the beginning of polymerization. The impedance spectra obtained are shown in a complex plane diagram, Fig. 28a, and as Bode-plots, Fig. 28b and c.

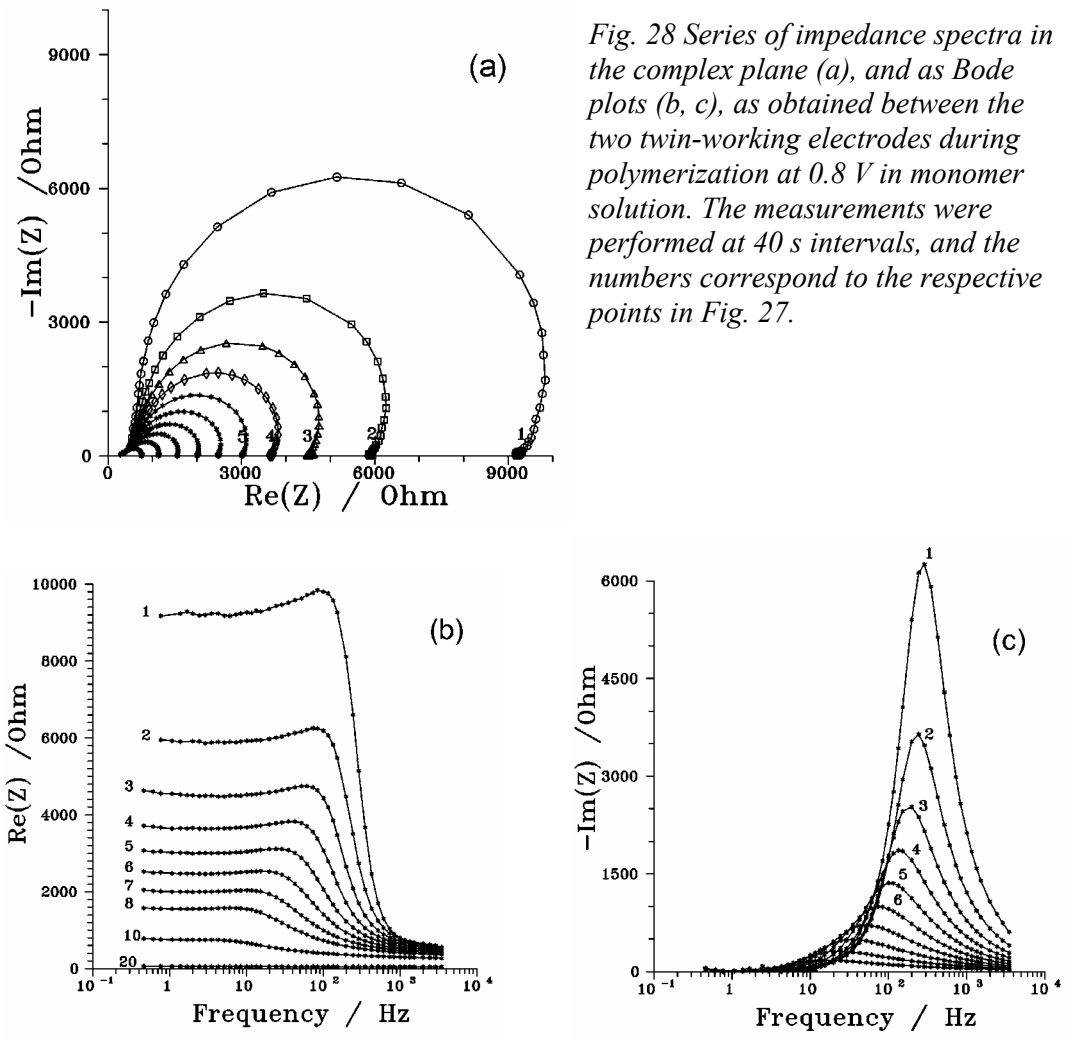

Fig. 28 Series of impedance spectra in the complex plane (a), and as Bode plots (b, c), as obtained between the two twin-working electrodes during polymerization at 0.8 V in monomer solution. The measurements were performed at 40 s intervals, and the numbers correspond to the respective points in Fig. 27.

These results were used to extract data for the dependence of the polymer resistance on polymerization charge as depicted in the picture below.

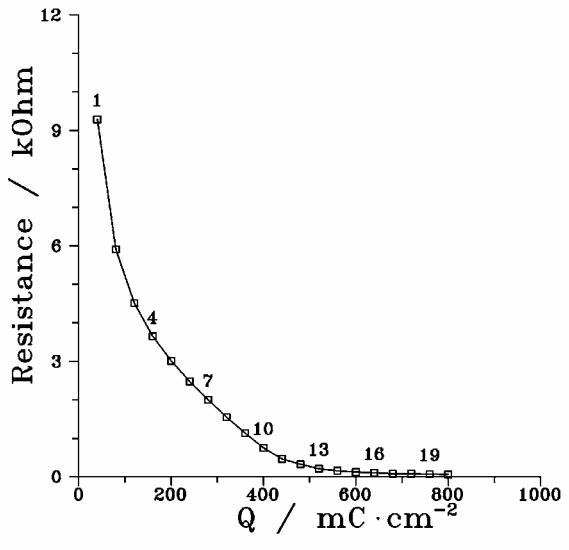

Fig. 29 Resistance data, extracted from the low frequency region of the impedance spectra, presented in Fig. 28.

4.2.3 Estimations of conductivity and thickness of the polymer layer

The resistance data, obtained from impedance measurements between the bands of the twin electrode during electropolymerization, can be used for estimation of specific resistance of the deposited polymer layer as shown in chapter 3.2. For this purpose the resistance data from Fig. 29 has been converted into conductance and presented versus logarithm of charge, used for deposition of the particular layer as follows:

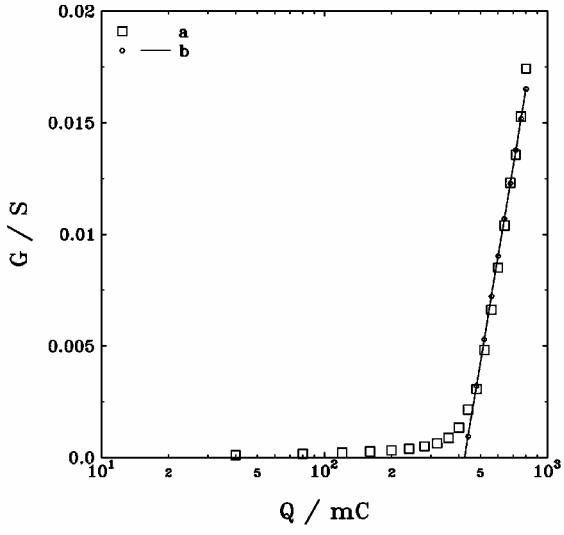

Fig. 30 (a) Conductivity data obtained from impedance spectra measured during the electrodeposition of polybithiophene vs. logarithm of charge, used for deposition; (b) fit of experimental data by eqn. 13 using dimensions of the twin electrode as in Fig. 5 and σ*=0.273 S·cm*$^{-1}$*, k= 0.011* μ*m mC*$^{-1}$*.*

It can be seen, that at the beginning of deposition no linear dependence of G on logarithmic charge is observed. That can be explained through an absence of an even bridging of a gap between the bands of the twin-electrode by the growing polymer layer. For thicker layers the conductance becomes linear dependent on the logarithm of charge according to eqn. 13. Hence, the values of the specific conductance of polymer layer σ and the thickness growth coefficient, k, related to 1·cm^2 electrode interface, could be estimated as 0.27 S·cm^{-1} and 0.011 μm mC^{-1} respectively. The thickness of the layer deposited upon a polymerization charge of 800 mC·cm^{-2} has been found to be 8.8 μm.

4.3 The thickness dependence of the impedance spectra of polybithiophene layers measured under galvanostatic condition

The electrochemical properties of conducting polymer layers are strongly dependent on their structure. The analysis of impedance spectra for polymer layers of different thickness in view of a particular physical model allows to prove or to refute the structural deliberations, laying in its basis. If the impedance dependence on thickness, predicted by the model (cf. chapter 3.1.2), take place, an estimation of the kinetic and thermodynamic parameters, common for the layers of different thickness, becomes possible.

As known from literature [32-36], the electrosynthesis of polybithiophen starts with initial formation of a dense polymer layer on the electrode substrate, but thicker layers have porous structure. Under the assumption, that the thermodynamic properties of polybithiophen do not depend on the layer structure, a combined analysis of thin and thick polymer layers is possible. Thereby, it was interesting to investigate very thin polymer layers, for which the simplified model (chapter 3.1.2) can be used and then to apply the evaluated parameters to analysis of thicker layers, for which the porosity has to be considered in addition. The EIS spectra, required for such investigation, were obtained using electrodes covered with both thin and thick polymer layers performing the impedance measurements under galvanostatical conditions.

4.3.1 Measurement results

Two series of EIS measurements were performed during galvanostatic polymerization of bithiophene. In the first one, the polymerization was curried out at relatively low current density of 0.15 $mA \cdot cm^{-2}$ in order to slow down the deposition rate and thus allow impedance spectra measurements at early stages of polymer growth. The recorded electrode potential vs. time dependence is shown in Fig. 31.

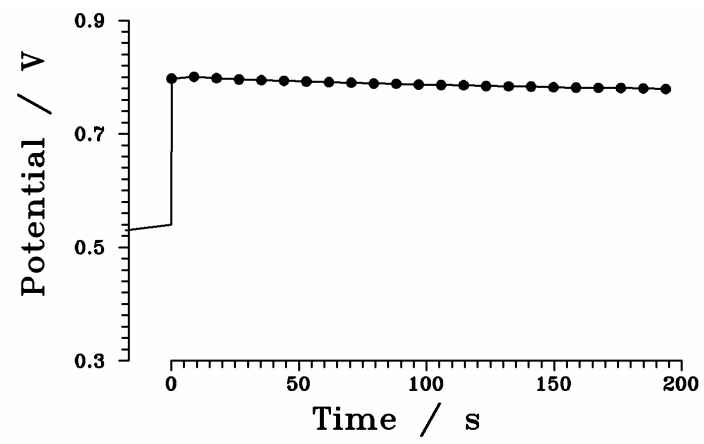

Fig. 31 Potential vs. time curve, obtained during electropolymerization of bithiophene at 0.15 mA·cm^{-2}. Impedance spectra measured as marked with dots.

The potential of the working electrode increases abruptly to a value of about 0.79 V and does not change considerably even upon prolonged polymerization. The EIS measurements were performed in 5 s intervals as marked in the figure. The obtained impedance spectra are shown as Bode-plots in Fig. 32 a, b. and the 5th spectrum is presented as a Nuquist plot in Fig. 32, c.

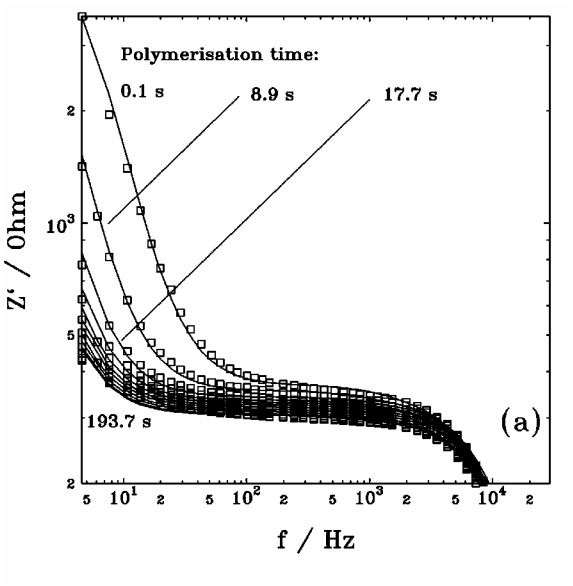

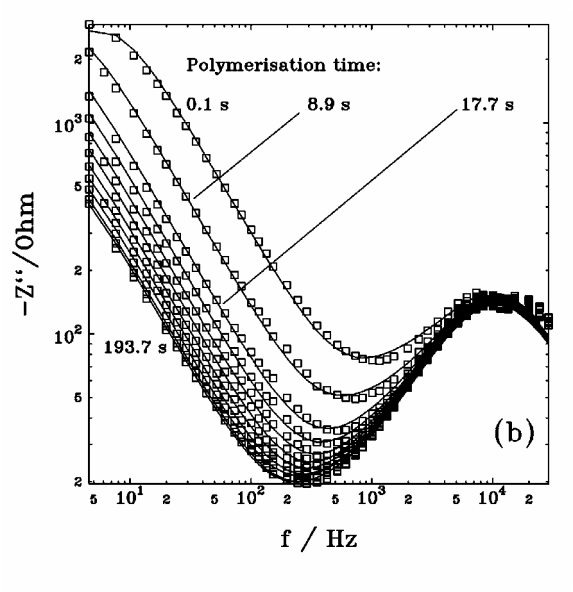

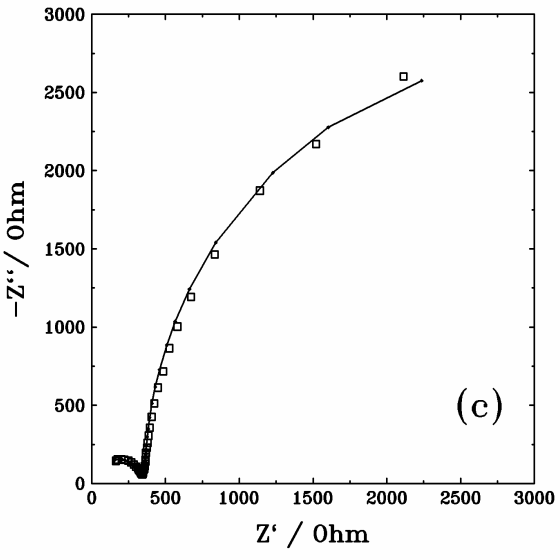

Fig. 32 A series of impedance spectra obtained during galvanostatically electropolymerization of bithiophene at 0.15 mA·cm^{-2} and the fits made using Ho et al. model, presented as Bode plots (a,b) and the 5th spectra as a Nuquist plot (c).

In a second experiment the polymer layer was deposited at a higher rate with current density of 2 $mA \cdot cm^{-2}$. The EIS measurements were performed at intervals of 15 s. In order to avoid polymer deposition during the impedance measurements, the cell current was switched to 0.0 $mA \cdot cm^{-2}$ for the duration of the perturbation pulses and respective data transmission to computer. The impedance spectra obtained are shown below as Bode plots. The total polymerization charge reached during this experiment was 450 $mC \cdot cm^{-2}$.

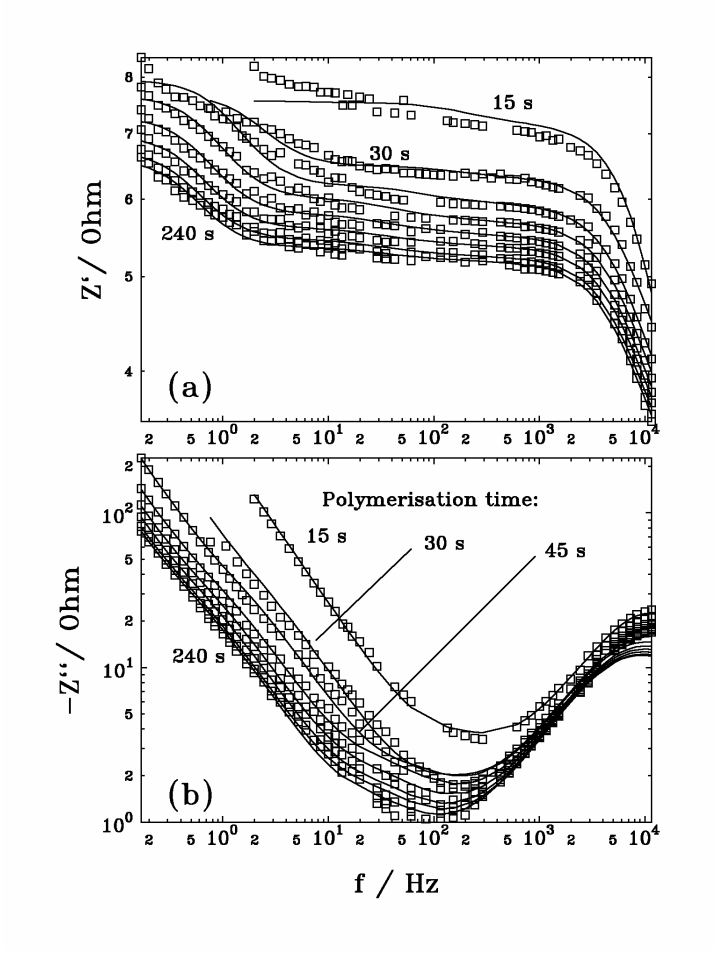

Fig. 33 A series of impedance spectra, measured during the polybithiophene layer deposition by polymerization current of 2 $mA \cdot cm^{-2}$. Solid lines represent the fit of the experimental data using the Paasch et al. model.

4.3.2 Data processing

The impedance spectra measured during polymerization at 0.15 $mA \cdot cm^{-2}$ were analyzed using the model of Ho et al. [48]. A second charge transfer resistance, R_p, has been introduced to account for the polymerization reaction. The eqn. 6 thus can be rewritten to give:

$$Z_1 = \left[\left(\frac{1}{Z_{nW} + R_{ct}} + i\omega C_{dl} + \frac{1}{R_p} \right) \cdot S \right]^{-1} + R_s \qquad \textit{eqn. 25}$$

where R_{ct} is the oxidation/reduction charge transfer resistance, C_{dl} is the double layer capacitance, S is the surface area of the electrode and R_s is the serial resistance. CNLS fitting of experimental data by use of eqn. 25 yielded the impedance spectra shown in Fig. 32. The thickness of the polymer layer obtained after passing 30 $mC \cdot cm^{-2}$ polymerization charge was estimated to be 80 nm using the value for polymer density ρ = 1.5 $g \cdot cm^{-3}$**,** as reported by Koßmel et al [30]. The value of dE/dc = 299.9 $V \cdot cm^3$ (cf. eqn. 5), determined from the fit of EIS data obtained for 30 $mC \cdot cm^{-2}$ layer, was assumed to be constant during polymerization and has been used further to estimate the polymer layer thickness for different values of polymerization charge passed as shown in Fig. 34a.

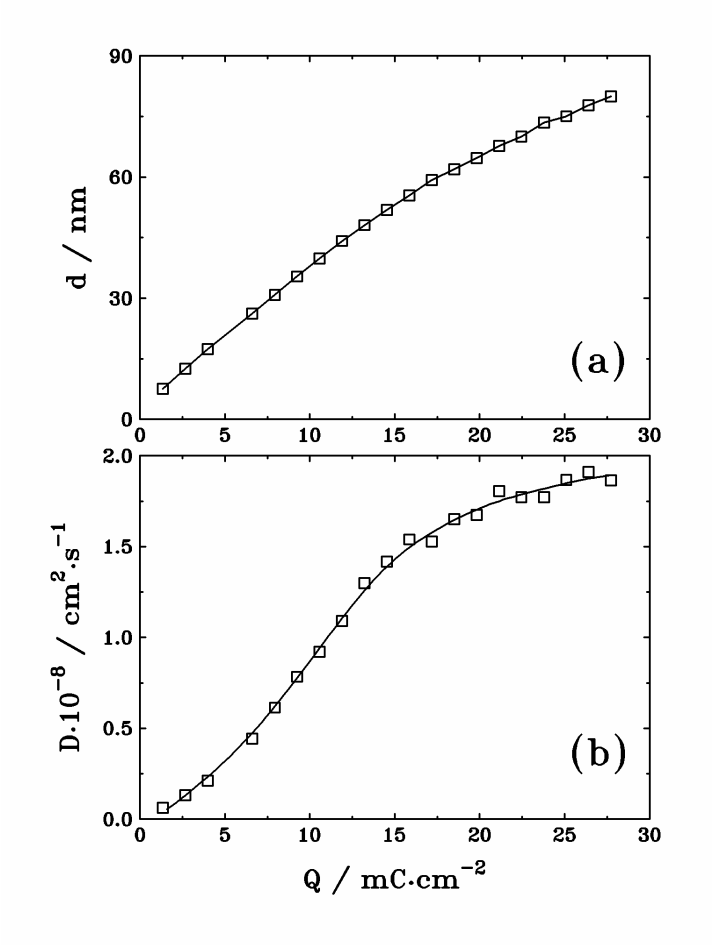

Fig. 34 Thickness of polymer layer and apparent diffusion constant, vs. polymerization charge passed during the polymer deposition at current density 0.15 mA·cm^{-2}.

The estimated values for the apparent diffusion constant of counterions, D, are shown in Fig. 34b. In the region, where the apparent diffusion constant becomes independent of the layer thickness and therefore Ho et al. model is valid, the diffusion constant D was determined as $1.8 \cdot 10^{-8}$ cm$^2 \cdot$s^{-1}. The values for R_p, C_{dl} and R_{ct} obtained from the fits are presented in Fig. 35.

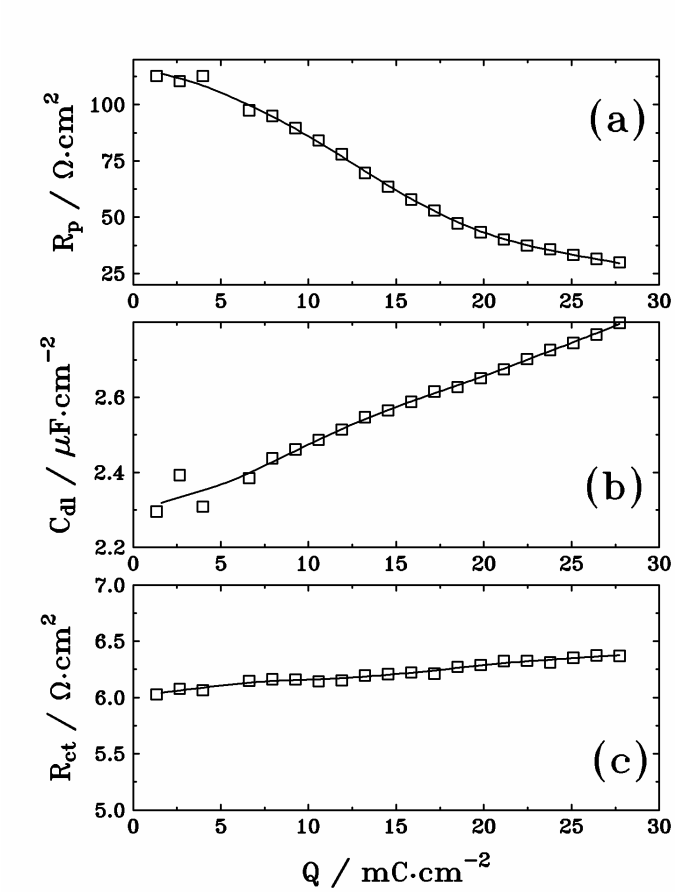

Fig. 35 Charge transfer resistance of polymerization reaction (a), double layer capacitance (b) and charge transfer resistance of oxidation/reduction of polybithiophene layer (c) vs. polymerization charge passed during the polymer deposition at current density of 0.15 mA·cm^{-2}.

The treatment of the impedance data measured on polymer layers consecutively deposited at a polymerization current of 2 mA·cm^{-2} was performed using the simplified model of Paasch et al (eqn. 9). The values of dE/dc, R_{ct} and the diffusion constant of counter ions D were assumed to be invariable and equal to the values estimated in the experiment with thin polymer layers. The value of diffusion length l of the counter ions could thus be evaluated from the fits as in Fig. 36a.

The assumption of a constant R_{ct} value allowed to estimate the effective interface of polymer, accessible for electron transfer. The effective interface coefficients obtained by fit of experimental data are shown on Fig. 36b.

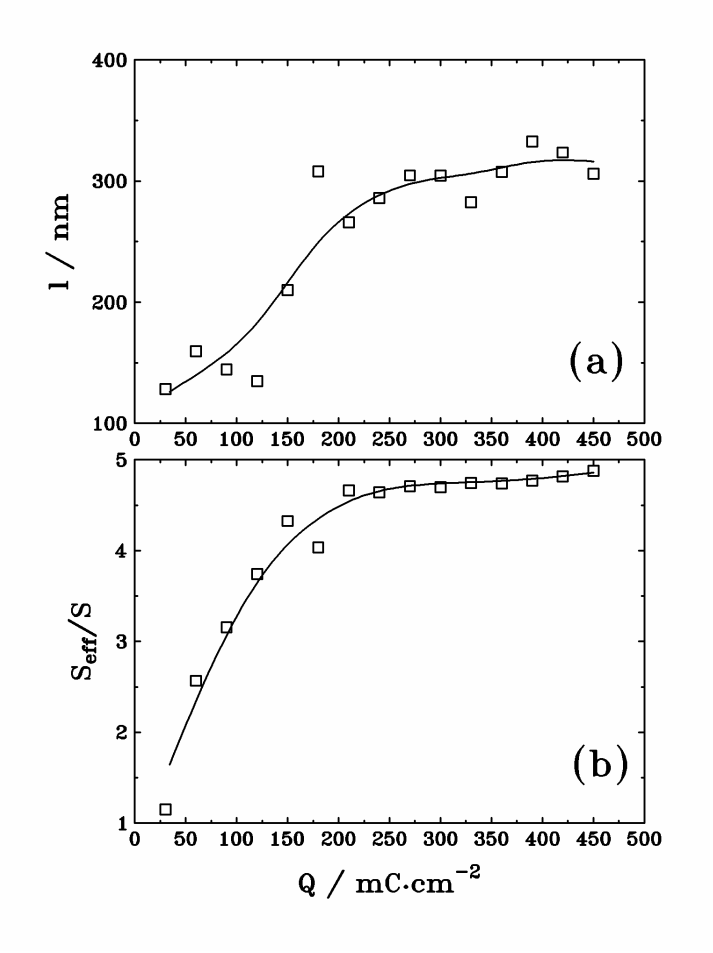

Fig. 36 Specific diffusion length (a) and effective interface coefficients vs. polymerization charge passed during the polymer deposition by current 2 mA·cm^{-2}.

The value of the effective diffusion length increases with the thickness of the polymer and saturates for polymerization charges > 200 $mC \cdot cm^{-2}$. Thus the region of validity of the model of Paasch et al. could be determined (Q > 200 $mC \cdot cm^{-2}$) and the thickness of polymer layer, the double layer capacity and the specific resistance could be evaluated, applying this model to the experimental EIS data obtained.

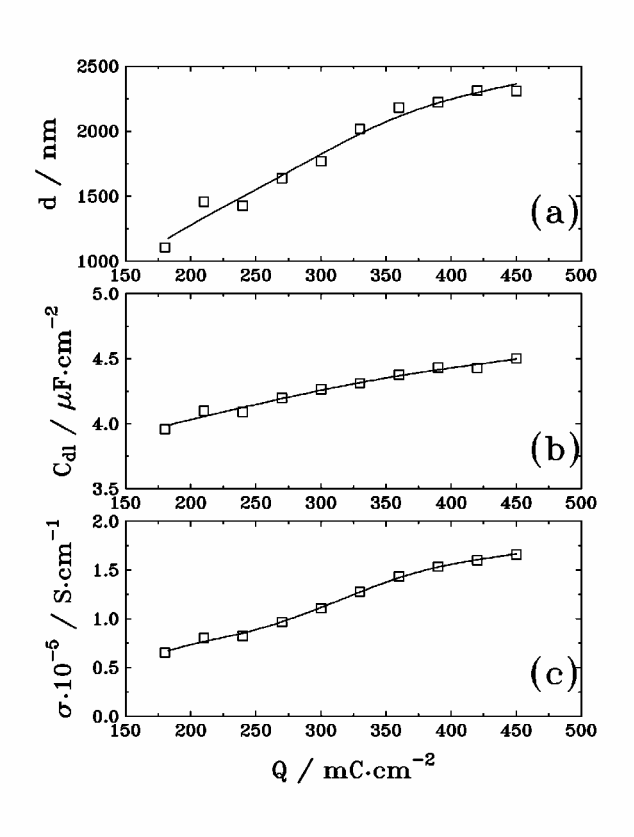

Fig. 37 The thickness of the polymer layer (a), double layer capacity (b) and sum of ionic and electronic conductivities of polybithiophene layer (c) vs. polymerization charge passed during the polymer deposition at current 2 $mA \cdot cm^{-2}$.

4.4 Impedance investigation of conducting polymer layers considering their inhomogeneity.

4.4.1 Model of an inhomogeneous porous electroactive layer

Experiments described in this thesis as well as data from the literature [9,25] show, that electrodeposited polymer layers are porous and behave as a two-phase system. The model of Paasch et al. is based on the assumption of macrohomogeneity of the polymer layers and allows good description of their impedance spectra in the oxidized state. However, the observed impedance spectra of polymers in reduced state, presented in the complex plane, exhibit a slope between 50 and 70 degree in the lower frequency range (cf. Fig. 15), which can not be descibed by the model of Paasch at al. One of the possible reasons for such a behavior could be inhomogeneity of the polymer layer in the direction perpendicular to the electrode interface. The analysis of the polymer layers of different thickness also prove the reliability of this assumption. Thus, a model taking into account both porosity and macroinhomogeneity was developed as an improvement of the Paasch et al. model.

We consider a polymer layer with thickness d to be divided by cross-sections with surface S into N sublayers, each with thickness $\Delta d = d/N$, as shown in the scheme below.

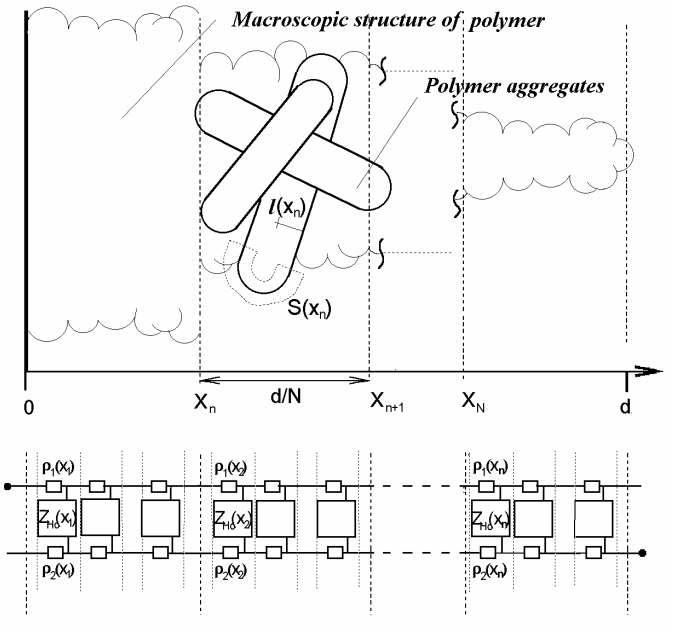

Fig. 38 Scheme presenting the dividing of macroscopic polymer layer into elementary volumes and the network consisting of chain connected transmission lines, describing the electrical behavior of such a system. l(x) is the characteristic diffusion length and S(x) the effective interface of the elementary volume with recession x from electrode.

The resulting polymer sublayers are assumed to be described by parameters. functionally depending on the distance from the electrode. The total number of the cross-sections has to be high enough, so that additional division does not effect the value of input impedance considerably.

The electrical response of every layer is presented by a transmission line as proposed by Paasch et al (cf. Fig. 9). It is assumed, that the polymer layers, which consist of polymer and electrolyte, included in pores, are connected polymer to polymer and electrolyte to electrolyte. Thus, the total impedance of such a structure corresponds to a cross-contacted network of chain connected transmission lines. An important simplification for the calculation of the total impedance of the considered equivalent circuit can be reached, if the electronic or ionic conductances can be neglected, yelding an infinitely conducting line on the corresponding side of the circuit (Fig. 10). The above made assumption about the connection between the elementary layers as polymer-to-polymer and electrolyte-to-electrolyte has a consequence, that the infinitely conducting line of each element is connected to the infinitely conducting line of the next element. In this case the measurements with cross-contacted and direct-contacted network give equal total impedance and therefore the circuit shown in Fig. 38 can be rearranged as follows:

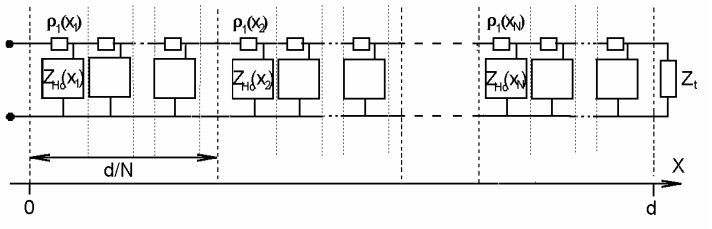

Fig. 39 The equivalent circuit describing an inhomogeneous in the x-direction polymer layer, where either electronic or ionic resistance can be neglected. $Z_t = \infty$ for the case of conventional impedance measurement and $Z_t = 0$ for measurement of a layer, contacted on the one side.

The terminating impedance Z_t can be either infinite to describe the case of conventional impedance measurement or zero to represent the impedance of electrode-polymer-electrode or electrode-electrolyte-electrode connected polymer layer. An expression for the impedance of such a network can be derived by technique, common in electronic engineering.

The required input impedance on the left gate of a homogenous transmission line is determined by the terminating impedance on it right gate and the characteristics of the line. Now, we have a chain of transmission lines with different parameters. The input impedance of the first one $Z_i(1)$ is the required input impedance of the whole network. Every elementary transmission line from left to right has as terminating impedance, $Z_t(n)$, the input impedance of the next one, $Z_i(n+1)$, which is unknown. We know only the impedance Z_t terminating the last of them. Therefore the solution for the first input impedance can be found by "transmission" of the terminating impedance at the end of the network through all of the homogenous transmission lines.

It can be shown [*61*], that a dependence of the input impedance Z_i of a homogenous transmission line of length Δd on the terminating impedance Z_t is given by

$$Z_i = Z_0 \frac{1 + \frac{Z_t/Z_0 - 1}{Z_t/Z_0 + 1} e^{-2\gamma \Delta d}}{1 - \frac{Z_t/Z_0 - 1}{Z_t/Z_0 + 1} e^{-2\gamma \Delta d}} \qquad \textit{eqn. 26}$$

Here, $\gamma \equiv \sqrt{\frac{\rho'}{Z'_{Ho}}}$ is commonly called the *propagation coefficient* and $Z_0 \equiv \sqrt{\rho' Z_{Ho}}$ is denoted as *characteristic impedance* of the transmission line.

To simplify further treatment, it is expedient to introduce the so called *reflection factor* on the beginning of the transmission line, r_i, and the terminating *reflection factor* on the end of transmission line r_t.

$$r_i = \frac{Z_i/Z_0 - 1}{Z_i/Z_0 + 1} \qquad r_t = \frac{Z_t/Z_0 - 1}{Z_t/Z_0 + 1} \qquad \textit{eqn. 27}$$

The eqn. 26 can be then rewritten as

$$Z_i = Z_0 \frac{1 + r_t\, e^{-2\gamma \Delta d}}{1 - r_t\, e^{-2\gamma \Delta d}} \qquad \textit{eqn. 28}$$

Comparing eqn. 27 and eqn. 28 can be seen, that the input reflection factor is related to the terminating reflection factor by the simple expression

$$r_i = r_t\, e^{-2\gamma l} \qquad \textit{eqn. 29}$$

Now we have to evaluate the terminating reflection factor of the *n*th line, through the terminating reflection factor of the *(n+1)*th line. As mentioned above, $Z_t(n)=Z_i(n+1)$. Thus, if we substitute the $Z_i(n+1)$, expressed through the terminating reflection factor of the *(n+1)*th line, as in eqn. 28, into eqn. 27 we get

$$r_t(n)=\frac{(Z_0(n+1)-Z_0(n))+r_t(n+1)e^{-2\gamma(n+1)\Delta d}(Z_0(n+1)+Z_0(n))}{(Z_0(n+1)+Z_0(n))+r_t(n+1)e^{-2\gamma(n+1)\Delta d}(Z_0(n+1)-Z_0(n))} \qquad \textit{eqn. 30}$$

Now through consecutive calculating $r_t(n)$ beginning from the last chain $r_t(N)$ we can evaluate the reflection factor for the first chain and therefore the required input impedance of the whole network. The terminating reflection factor of the last chain, $r_t(N)$, can be directly calculated by substituting the value of terminating impedance Z_t into eqn. 27. As mentioned above, $Z_t= \infty$ and $Z_t = 0$ are the cases interesting for impedance measurements on conducting polymers. The terminating reflection factors for the last chain are correspondingly $r_{t\,\infty}(N) = 1$ and $r_{t\,0}(N) = -1$

A close mathematical expression for the input impedance of the considered network can be found for the case of small inhomogeneity over the distance Δd. In this case an equality of the characteristic impedances Z_0 of the adjoining transmission lines can be assumed. A substitution $Z_0(n) = Z_0(n+1)$ into eqn. 30 gives:

$$r_t(n)=r_t(n+1)e^{-2\gamma(n+1)\Delta d} \qquad \textit{eqn. 31}$$

The consecutive substitution of every $r_t(n+1)$ until end of the line gives the terminating reflection factor of the first chain for the cases of the open-circuit and the case of the short-circuit respectively as:

$$r_{t\,\infty}(1)=\exp\left[\sum_{n=0}^{N}-2\gamma(n)\Delta d)\right] \qquad r_{t\,0}(1)=-\exp\left[\sum_{n=0}^{N}-2\gamma(n)\Delta d)\right] \qquad \textit{eqn. 32}$$

Substitution of these reflection factors into eqn. 27 gives expressions for the input impedance of the first chain for both cases

$$Z_{i\infty} = Z_0(0)\frac{1+\exp\left[\sum_{n=0}^{N} -2\gamma(n)\Delta d\right]}{1-\exp\left[\sum_{n=0}^{N} -2\gamma(n)\Delta d\right]} \quad Z_{i0} = Z_0(0)\frac{1-\exp\left[\sum_{n=0}^{N} -2\gamma(n)\Delta d\right]}{1+\exp\left[\sum_{n=0}^{N} -2\gamma(n)\Delta d\right]} \qquad \textit{eqn. 33}$$

This expressions can be rewritten using hyperbolic functions as

$$Z_{i\infty} = Z_0(0)\coth\left[\sum_{n=0}^{N} -2\gamma(n)\Delta d\right] \qquad Z_{i\infty} = Z_0(0)\tanh\left[\sum_{n=0}^{N} -2\gamma(n)\Delta d\right] \qquad \textit{eqn. 34}$$

It can be seen, that this expressions go over into the well known expressions for the impedance of the homogeneous transmission line (cf. eqn. 9) if all the γ(n) are equal. The ability of this approximate solution to describe the behavior of real conducting polymer layers will be discussed further in this work.

The proposed mathematical solution can correctly describe a network with any arbitrarily set parameters for all sublayers. However, for a physically relevant model of conducting polymer layers, only smooth dependence of the parameters on the distance to the electrode can be considered. Using a function describing the expected dependence and fitting its parameters instead of the parameters of each sublayer can greatly improve the efficiency of the fitting procedure. The choice of such function can be different for every special case. A function, further refered as *inhomogeneity function*, can be used to describe the uniform decrease of sublayer parameters with the distance from electrode.

$$p(x) = p_0\frac{1-e^{k(d-x)I}}{1-e^{k\,d}} \qquad \textit{eqn. 35}$$

Here x is the distance from the electrode and d the thickness of the polymer layer. The parameter value change from p_0 (*scale factor*) to zero over the interval d. The product k·d can be treated as a *form factor*, which controls the decrease of the parameter. Its change from -∞ to ∞ causes the change of the parameter dependence on the distance as shown in Fig. 40.

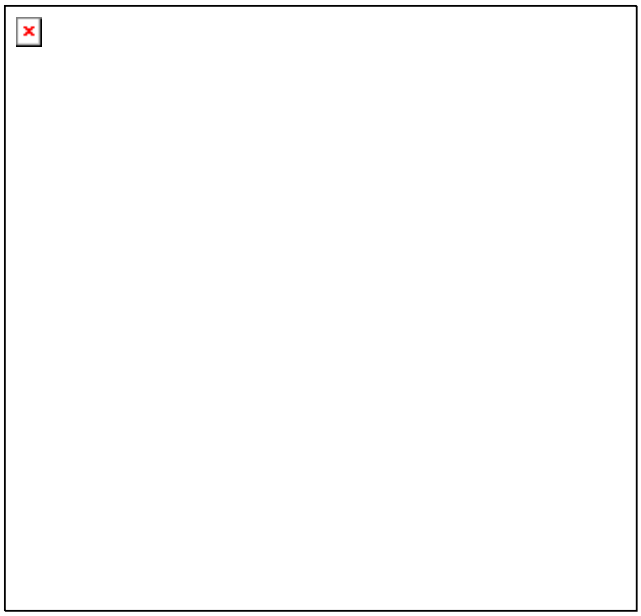

Fig. 40 Parameter dependence on distance x from the electrode as described by the inhomogeneity function for different values of the form factor. Values of p_0=1 and d=10 were used to simulate p(x) using eqn. 35

It should be mentioned, that performing numerical calculations of reflection factor for a value of parameter equal to zero is unreasonable and hence the calculation for the *N*th layer was not carried out. The practical consequence of this approach is the absence of inhomogeneity for parameters having a form factor < -1000.

4.4.2 Experimental results and validation of the model

The model described above was applied to impedance spectra measured on polybithiophe layers in different oxidation state, aiming to investigate the character of their inhomogeneity. The impedance measurements were performed in steady state conditions on polybithiophene layers, electrodeposited by total charge flow of 80 $mC \cdot cm^{-2}$, in an electrolyte solution, free from monomer. The resulting impedance spectra are presented below as Bode plots.

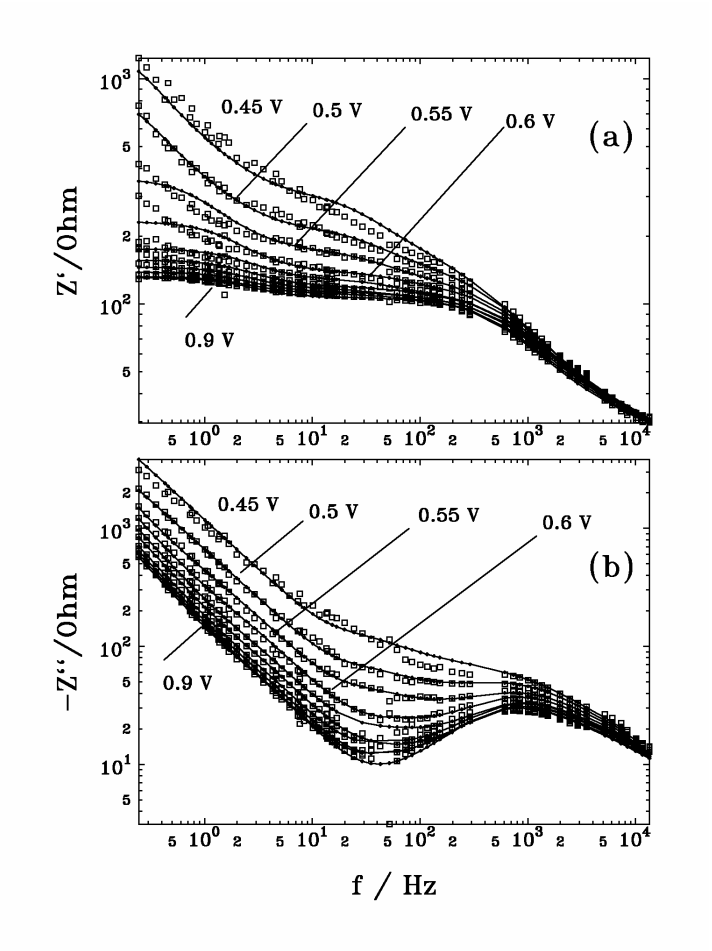

Fig. 41 A series of impedance spectra of polybithiophene layer at different potentials in steady state (a) real part, (b) imaginary part vs. frequency. Solid lines corresponds to CNLS-fit of experimental data by use of eqn. 30 with N=50

The critical number of cross-sections needed to provide the condition, mentioned above, that the simulated impedance spectra should not further change with increasing N, must be estimated experimentally for every particular set of parameters. In general, the strong inhomogeneity necessitates a large number of cross-sections. In our case this conditions was fulfilled by N = 50 even for cases of strong inhomogeneity. As can be seen in Fig. 42 below, the difference between the spectra calculated with N more than 20 becomes negligibly small for the set of parameters describing the layer of a reduced polymer, where the inhomogeneity of the resistance reaches its maximal value.

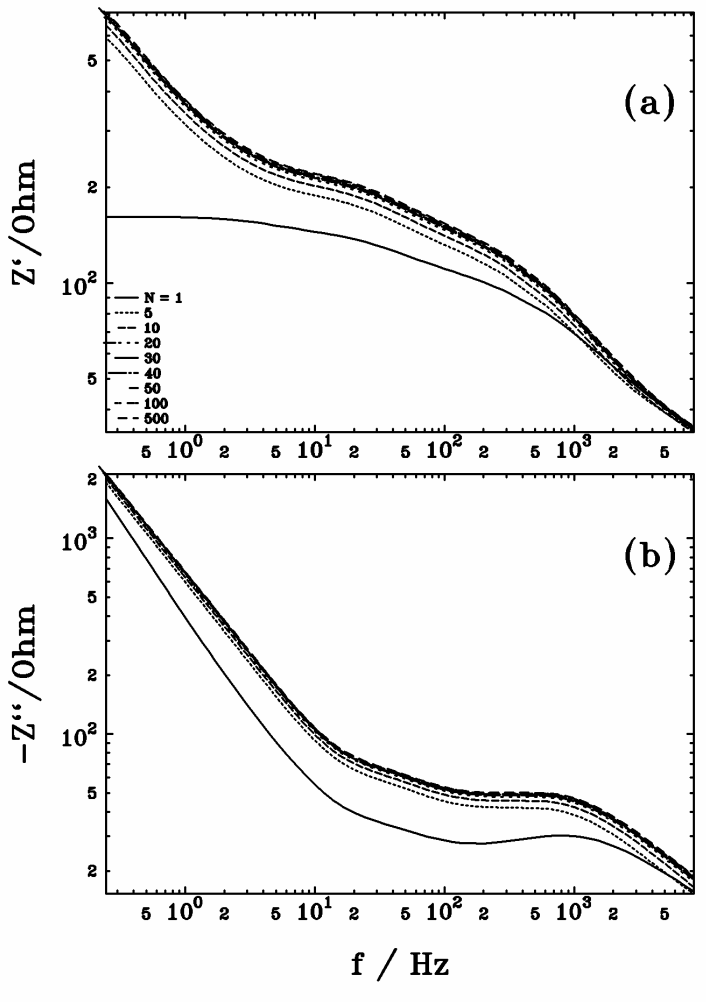

Fig. 42 Impedance spectra simulated by use of eqn. 30 for different numbers of cross-sections, N. The set of parameters, optimized to describe the experimental spectra measured by 0.5 V has been used for the simulation.

Using the approximate solution for the impedance of inhomogeneous polymer layer, given by eqn. 34, could considerably simplify the numerical optimization, carried out to fit the experimental data. However, the justification for use of this equation is based on the assumption of small inhomogeneity over the length of one elementary section and is dependent on the particular set of parameters. A comparison of impedance spectra simulated with both the strict (eqn. 30) and approximate (eqn. 34) solution using same parameters calculated from the experemental data is shown in Fig. 43.

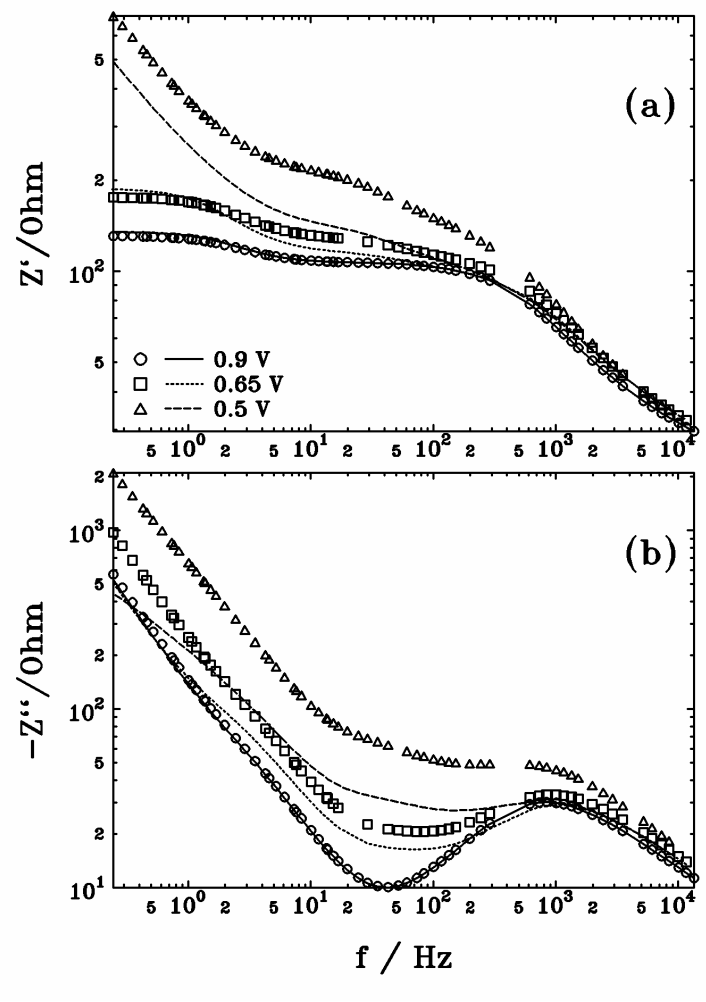

Fig. 43 Simulated impedance spectra using the parameters, optimized to fit to experimental data measured at electrode potential 0.9, 0.65 and 0.5 V. Lines - simulation by use of the approximate solution (eqn. 8) and markers - simulation by use of strict solution (eqn.5)

The set of parameters were optimized to describe the experimental data at different electrode potentials by use of the strict solution (eqn. 30). The obtained set of parameters was then used to compute the spectra by the approximate solution (eqn. 34). It can be seen, that the obtained spectra are in a good agreement with the exact calculated spectra only in the case of well oxidized polymer (0.9 V), where the inhomogeneity, required to describe the experimental data, is small. Therefore, the analysis of the experimental data was further performed by use of the strict solution for the impedance at all electrode potentials.

The number of the parameters to be optimized could be reduced by use of the values for dE/dc, D and R_{ct} estimated in 4.3.2 for thin polymer layers, which can be considered as non porous and homogeneous. These values were used as fixed parameters to fit the impedance spectrum measured on oxidized layer (0.9 V) and allowed evaluation of the polymer layer thickness as well as of the scale factors for the effective surface coefficient f_0 and characteristic diffusion length l_0 by fixed form factors $k_f d$ and $k_l d$.

The inhomogeneity of l and f parameters is characteristic for the structure of any particular polymer layer and therefore should be independent on the potential. This consideration allows to reduce the number of optimized parameters by assuming *constant* values for the form factors for l and f for *all* oxidation levels. The inhomogeneity functions satisfying this criterion were estimated by fit of series of experimental impedance spectra, as shown in Fig. 41. The curves representing the dependence of the specific diffusion length l and efective surface coefficient f on the distance from electrode are presented below.

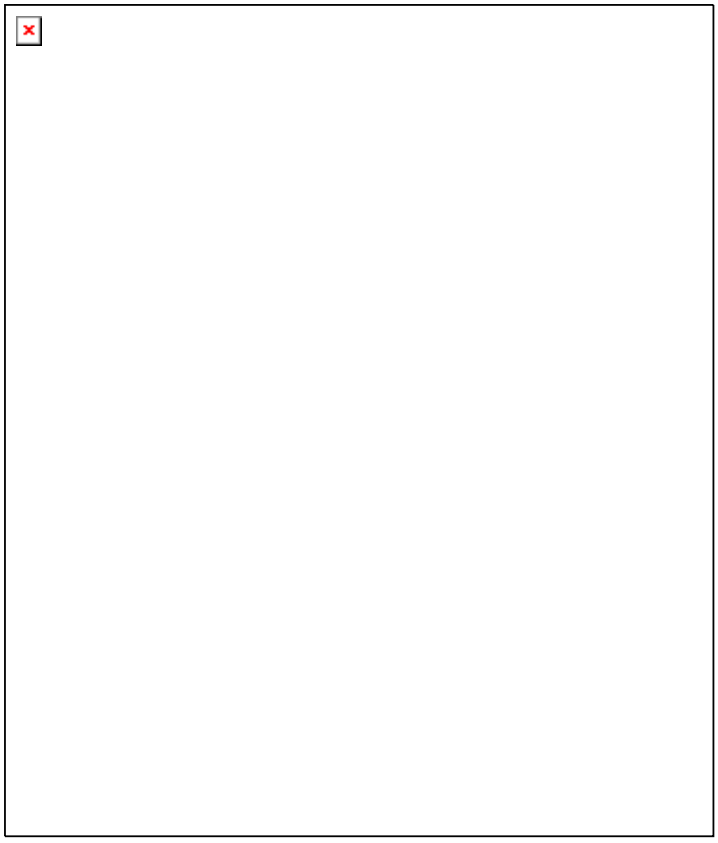

Fig. 44 Inhomogeneity profiles of characteristic diffusion length l (a) and effective surface coefficient f (b), which allow good fits of impedance spectra of polybithiophene layers for all oxidation potentials.

In contrast to the structural parameters *l* and *f*, the inhomogeneity of the specific conductivity can increase during prolonged reduction due to slow relaxation processes in polymer. Thus, the form factor of this parameter was set free in the fit of the experimental impedance spectra at different potentials. The resulting inhomogeneity profiles are shown in Fig. 45

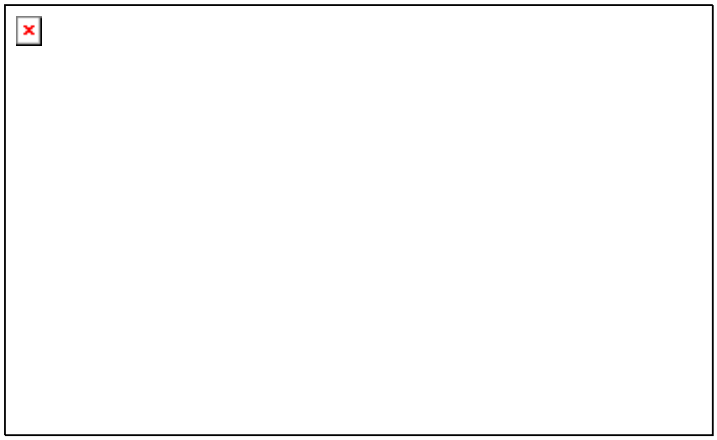

Fig. 45 Inhomogeneity profiles of the specific conductivity of polybithiophene layer at different electrode potentials.

The double layer capacity and charge transfer resistance, related to the effective interface of polymer, are presented in Fig. 46a and 46b, respectively. The change of dE/dc with electrode potential can be seen in Fig. 46c.

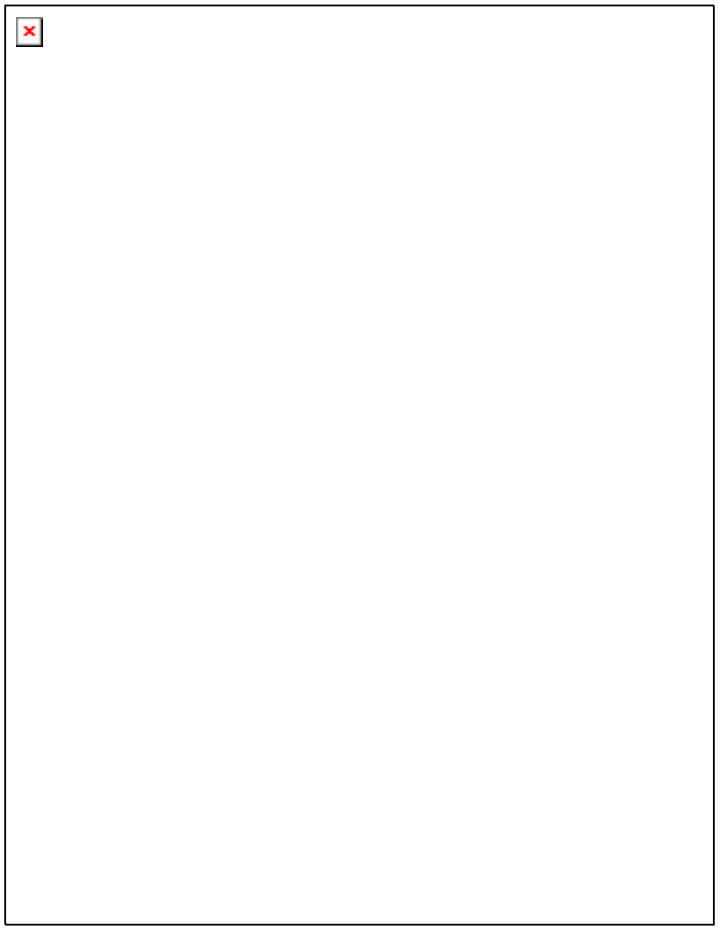

Fig. 46 Charge transfer resistance, R_{ct}, (a), double layer capacity, C_{dl}, (b) and dE/dc (c), evaluated by fit of series of impedance spectra, measured at different potentials, using eqn. 30.

The form factor of the inhomogeneity function of the resistance was found to change much more significantly with the reduction of polymer then the scale factor, in this case the resistance of the first layer. Thus, aiming to improve the efficiency of the fitting procedure, the resistance of the first layer was assumed to be constant during the first stages of reduction and was fixed at $2.4 \cdot 10^6$ Ohm·cm^{-1}. The apparent specific resistance of the whole layer, estimated by integration of the inhomogeneous resistance and dividing by layer thickness, is shown in Fig. 47a vs. electrode potential. The apparent diffusion constant of dopant in the polymer particles is presented in Fig. 47b.

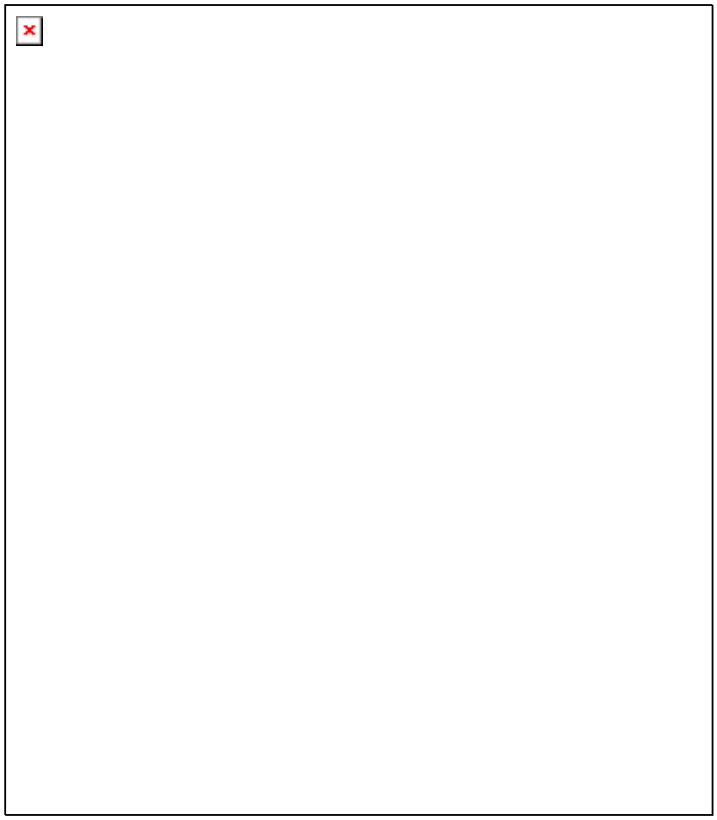

Fig. 47 Apparent specific resistance of the polymer layer, ρ, (a), and the apparent diffusion coefficients of the dopant ions, D, (b), vs. applied electrode potential

5 Discussion

5.1 The contribution of faradaic currents in the oxidation/reduction of polybithiophene and polypyrrole during cyclic voltammetry experements.

The combined analysis of CVs and impedance spectra, performed by Tanguy et al [9,25], has demonstrated the ability to distinguish between different processes, determining the redox behavior of conducting polymers. Their results are based on impedance measurements, performed in steady state. The results of our measurements have shown, however, that the impedance spectra are dependent not only on potential but also on time, due to the slow relaxation processes observed during oxidation and reduction. Thus, scan rate dependence should be expected in cyclic voltammetry measurements. The application of FFT-impedance spectroscopy allows impedance measurements during the potential sweep, so the measured impedance spectra correspond to the actual state of polymer layer and can be used for simulation of CVs.

Several recent reports have dealt with interpretation of the impedance spectra of polymer films deposited on metal electrodes [6,27,liv,*62-66*]. Some authors [6,62,63] apply the model of Ho et al. [48], assuming that at high frequencies charge transfer dominates, leading to a semicircle in the complex impedance diagram, at intermediate frequencies the diffusion of ions determines the impedance leading to a Warburg-type behavior and at low frequencies to a highly capacitive behavior, due to the finite thickness of the polymer layer. Others [27,liv,64-66] have applied a transmission line model to take account for the porosity of the polymer layer.

The high frequency impedance behavior of an electrochemical cell does not influence its current-voltage characteristic at moderate scan rates and in the case of slow CVs, only the low frequency range must be considered. Thus, a simple equivalent circuit, represented by a resistor, R, and a series capacitor, C, can be justified experimentally by the observed vertical segment in the impedance spectra of oxidized polymer electrodes - cf. Fig. 15 and Fig. 16. This simplification results also from the model of Ho et al (see

eqn. 7) and the transmission line based model of Paasch et al (eqn. 10). Here, the quantities R and C have been only used for prediction of CVs using the results obtained from in situ EIS measurements on PPy and PBt covered electrodes. The actual physical parameters included in this apparent impedance elements have been analyzed by fit of the impedance spectra in the entire accessible frequency range and will be discussed in following sections.

The important question how to distinguish between faradaic and capacitive processes during a potential sweep experiment has been repeatedly discussed in the literature [21, 70-69]. Most of the authors emphasize the inseparability of the faradaic and the capacitive current components by electrical measurements. However, the definition of the notion "capacitive" is often not well determined, which additionally complicates the discussion. In this work the capacitive part of the current is defined *formally* as one of a serial capacitor as revealed from the impedance spectra. The actual meaning of C can be derived only from a physical model, for instance the one proposed by Ho et al (eqn. 7). With regard to this model, by subtraction of the current resulting from this capacity we actually exclude processes connected with the establishment of a chemical equilibrium between different redox species of conducting polymer and the recharge of the double layer. The remaining current, referred further on as *faradaic current*, can be due to overoxidation of polymer, solid state polymerization or reducing of some species, present in the electrolyte in small amount.

5.1.1 Polybithiophene.

The impedance spectra measured in situ for PBt covered electrode can be, to a good approximation, described by the assumed series connection of R and C in the potential ranges 0.6 V to 1.0 V in the anodic sweep and 1.0 V to 0.3 V in the cathodic sweep - cf. Fig. 15. The slope of the low frequency spectra segments is between 75^{o} and 85^{o} which supports the suggested simple equivalent circuit, applied for low frequencies. The impedance spectra obtained during an anodic sweep in the potential range 0.3 - 0.5 V can not be approximated by an R-C circuit. The analysis of such spectra can only be correctly performed taking into account the inhomogeneity of a polymer layer, as discussed in chapter 5.4. For the purpose of simulating CVs, however, the exact

determination of R and C in this region of potentials is not a matter of concern. The current in this potential range is low and hardly measurable, therefore no reliable comparison with the experimental data can be performed anyway.

As shown in Fig. 17, R changes significantly with the onset of oxidation during the anodic sweep, however, it changes only little during the cathodic sweep, even at reductive potentials. Similarly, the build-up of C can not be completed during the anodic sweep and continues to increase further during the reverse sweep, until the reduction becomes dominant at lower potentials (cf. Fig. 17). Such an effect has been observed even for steady state impedance measurements by Tanguy et al. [25]. They ascribe this phenomenon to a profound structural change of the polymer during oxidation. According to Heinze et al. [*70*] such structural relaxation processes should accompany the oxidation and reduction of conjugated materials, such as PPy and polythiophene. The delayed increase of the capacitance depends further on the sweep rate and this underlines once more the necessity of in situ impedance measurements during potential sweeps for the purpose of simulating cyclic voltammograms. According to eqn. 24, usually applied for calculation of the capacitive current during a potential sweep, it should be expected that the most significant capacitive effects on the current-voltage characteristics of a polymer film occur in the potential range where the capacitance has its highest values. A curve calculated using eqn. 24 is presented in Fig. 19b for comparison. However, as can be seen from the more general eqn. 23, the capacitive current should strongly depend on the derivative dC/dU and not only on the value of C(U). In cases where the capacitance of the sample significantly changes with the electrode potential (cf. Fig. 17), the capacitive part of the current can not be calculated using the simple eqn. 23. At a first look, the numerically computed capacitive current as depicted in Fig. 19a, seems to have a very strange potential dependence. High capacitive current flows at the onset of the oxidation of the polymer, an effect that is related to the increase of the sample capacitance in this potential range. It seems that the main contribution to the total current flow during the first stages of the oxidation and reduction is of capacitive nature as can be seen from the comparison of curves (a) and (c) in Fig. 17. At higher anodic potentials, 0.6 - 0.8 V, the capacitive current decreases, approaching $I_a=C(U)\cdot\upsilon$, because the capacitance of the polymer does not change

significantly in the range 0.9 - 1.0 V (cf. Fig. 17). After the sweep reversal, however, the capacitive current cannot approach the values predicted by eqn. 23, because of the further increase of the capacitance during the first half of the sweep, but remains low and even decreases further.

5.1.2 Polypyrrole.

EIS measurements of PPy covered electrodes were performed in situ in the potential range -0.4 V to 0.7 V in which the obtained impedance spectra can be described by the assumed series connection of R and C for low frequencies. The potential dependence of C and R is less pronounced, as compared with the PBt results and the capacitive current calculated from eqn. 23 shows a similar pattern as the curve obtained by using eqn. 24 instead, as can be seen in Fig.6. The faradaic current, obtained by subtraction of the calculated capacitive part, exhibits evidently different behavior in the two potential regions. It remains constant in the area under 0.4 V and begins to increase significantly above this potential. The current in the first potential region could be accounted for the solid state polymerization, which is imaginable to be connected with significant spatial difficulties and therefore not limited by the charge transfer (and potential). The faradaic current has an onset at 0.4 V and can either result from oxidation of some species present in the electrolyte or from overoxidation of the polymer.

5.2 Contribution of electronic and ionic resistance to the resistive hindrance of the recharge processes of polybithiophene

The impedance measurements with the twin electrode, presented in Fig. 12, were performed aiming to obtain the value of electronic conductivity of polymer layer independent on its ionic conductivity. The measurements, performed during anodic potential sweep in monomer-free electrolyte enabled the determination of the polymer layer impedance for different stages of oxidation. It was observed (cf. Fig. 23), that even in its highly conductive state the polymer layer exhibits complex impedance behavior. The impedance has however no imaginary components in the frequency range below 10 Hz and presents therefore pure electronic resistance of polymer. As it could be

expected, it decreases strongly during the process of oxidation, exhibiting a change of more than two orders of magnitude, as can be seen in Fig. 25.

The impedance spectrum shown in Fig. 26, obtained in a conventional three-electrode EIS measurement is typical for conducting polymers in the oxidized state and is well known from literature. The measurement was performed on the same sample and with no changes in electrochemical cell configuration, except that the two twin-working electrodes were externally connected with a wire. It can be seen that the extreme capacitive and blocking behavior of the polymer/electrolyte interface determines almost entirely the impedance spectrum of the sample. The influence of the polymer resistance can be seen on a slightly depressed character of the semicircle in the high frequency range, but is hardly to determine quantitatively. The measurements performed with a twin-working electrode allows, on the contrary, an exact evaluation of the electronic conductivity of polymer along with the information about the processes on the polymer interface.

During polymerization at a controlled anodic potential, the polybithiophene layer grows in its oxidized and conducting state [*71*,*72*]. The total electric charge passed through the cell is related to the number of monomer units oxidized and deposited as polymer layer on the electrodes and to the charge used in the process of the polymer oxidation. Thus, although indirectly, the curve presented in Fig. 27 characterizes the formation of an oxidized polymer layer during polymerization. The growth rate evidently increases with time due to the polymer layer porosity and the increase in active surface area.

In situ EIS measurements between the bands of the twin electrode has been performed during polymerization as marked with the numbered points. It can be seen from the obtained impedance spectra (cf. Fig. 28) that the gap of the twin- working electrode was already bridged with polymer before the first impedance spectrum has been measured, i.e. in less than 40 s polymerization time. A complete interpretation of the obtained impedance spectra can be given using an approach described in the chapter 4.4.1. and the knowledge of the field distribution between the bands of the twin-electrode. However, such a distribution for the case of the inhomogenous polymer layer is rather complicated and still remain a problem to be solved.

Some general features of the impedance spectra are evident, though. The Ohmic behavior for low frequencies, as seen in Fig. 28, can be attributed to electronic conduction through the polymer aggregates. Low frequency resistance data, obtained from Fig. 28b, are compiled in Fig. 29 to represent the dependence of the d.c. resistance on the polymerization time. Evaluation of specific resistance values, however, depends on particular electrode configuration. Model calculations, based on the electric field distribution between the two metal stripes of the twin-working electrode, were performed to gain insight into the dependence of the specific conductance between the bands of the twin electrode on the layer thickness. The assumption of a linear dependence of the layer thickness on the total charge used for polymerization had to be used to evaluate the values of the specific conductivity and thickness of the layer. The value of the specific electronic conductivity of the polymer has been found to be much higher as the conductivity determined from conventional impedance measurements, where ionic resistance has a significant effect. The analysis of the inhomogeneity of even much thinner polymer layers, presented in chapter 4.4.2, let imagine, however, that the assumption of the homogenous polymer layer, used in the the calculation of the specific resistance, does not satisfactorily match the real polymer structure. A field calculation taking into account the inhomogeneity of the polymer layer can be proposed as further step in the development of this investigation method.

5.3 Evaluation of kinetic relevant parameters of conducting polymers by analysis of layers with different thickness.

The formation of conducting polymer layers during the electropolymerization has been intensively investigated in the last years [14,32-38]. However, the potentiostatic measurements, commonly used for this purpose, do not allow to observe closely the first stages of the layer growth, due to the nonlinear dependence of the formation rate on potential at the onset of deposition. Thus, impedance measurements were performed during galvanostatic polymerization of bithiophene at low enough current density of 0.15 $mA \cdot cm^{-2}$. The absence of distortions of the potential response, due to changes in the polymer layer during the EIS- measurement were checked by analysis of obtained power spectra using an approach, described in [l]. Separation of two stages of layer

growth was possible in the time scale of the polymerization experiment using this current density, as obtained data have shown.

The use of the Macdonald's CNLS program for fitting the experimental data allowed comprehensive analysis of the fit quality. The relative standard deviations of parameters supplied by the optimization program are representative for the goodness of the entir fit as well as for the influence of each parameter on the function value. All of the above presented parameters had average relative standard deviations bellow 10%, whereas a random distribution of the deviations for each frequency point has been detected. This is a confirmation for a correct separation of parameters during the fit of the particular experimental data by the used model. The comparison of the fit curves in Nuquist and Bode presentation with the experimental data also verifies the reliable choice of fitting functions.

The application of the model of Ho et al. was performed, assuming thin polymer layers nonporous and homogeneous. However, the apparent diffusion constant of the counterions depends on the film thickness at the initial stages of polymerization (Fig. 34b), what can correspond to 3-D growth of polymer nuclei rather than existence of homogenous polymer film, assumed by the model. For polymerization charge > 20 $mC \cdot cm^{-2}$, the apparent diffusion constant becomes practically invariable and so the requirements for the use of Ho et al. model become fulfilled. That can be a consequence of a crossover to 2-D growth with a formation of homogenous polymer layer. The estimated diffusion constant for this region amounts to $1.8 \cdot 10^{-8}\ s^{-1} \cdot cm^2$. The charge transfer resistance (Fig. 34a) does not change significantly during the polymerization, indicating a constancy of the interface available for oxidation/reduction reaction of the polymer. The exchange current density corresponding to the R_{ct} value of the thickest film was estimated to be 4 $mA \cdot cm^{-2}$. The capacitance of the double layer obtained from the fits increases linearly with the film growth (Fig. 35b). This result shows, that the inner regions of polymer film are possibly also involved in the formation of double layer. The approximation of the obtained linear dependence to 0 polymerization charge, where the interface can be assumed equal to the geometrical, yields for the specific double layer capacitance the value of 2.4 $\mu F \cdot cm^{-2}$.

Increasing of the electrode interface covered with polymer or a lower activation energy for electron transfer from the monomer result in a decrease of the charge transfer resistance during the first stages of film growth (Fig. 35c). The latter can be due to the fact that the already deposited film is better substrate for polymer precipitation than Platinum. After a formation of a compact polymer layer the charge transfer resistance becomes nearly constant.

The use of the impedance equations proposed by Ho et al. and Paasch et al. in the form, including the structure independent layer parameter dE/dc, allows to perform a combined analysis of both thin and thick polymer layers. Independence of this parameter on the layer thickness requires only constancy of the polymer density inside of elementary polymer aggregates during the polymer growth. Such an assumption can be justified in view of the results of the polymer density measurements made by flotation method [*73*].

During the first stages of polymerization the characteristic diffusion length, resulting from fit of experimental data (Fig. 36a), changes with the film thickness, which does not prove the assumptions made in the model of Paasch et al. After deposition of polymer of up to 180 $mC \cdot cm^{-2}$ polymerization charge the characteristic diffusion length becomes constant. Similar behavior was reported by Tanguy et al. for methylthiophene [9]. The estimated value for the characteristic diffusion length (300 nm) let us conclude, that fibriles of polymer, for which similar dimensions are estimated by SEM measurements [*74*], are the regions where diffusion becomes the limiting step of charge transfer.

The effective surface coefficient increases with layer thickness until the polymerisation charge reaches the value of 250 $mC \cdot cm^{-2}$. The growth of the interface due to deposition of more polymer becomes then compensated by blocking of already accessable interface. This effect should result in macroinhomogeneities, that should be taken into account in the analysis of thicker polymer layers. The possible model approach for this case is discussed in the next chapter.

The estimated maximal effective surface is 4.7 times larger then the geometric surface of electrode. This value is much smaller than values estimated by adsorption experiments [*75*]. The observed difference could be explained by the assumption, that

organic molecules can adsorb inside of the polymer conducting areas whereas the electron transfer can occur only on their interface. The volume occupied by polymer aggregates can be estimated by multiplication of the effective interface and characteristic diffusion length. This volume amounts to 0.7 times the value of geometrical volume of the film, calculated from film thickness obtained by the fit (Fig. 37a) and can serve as a characteristic for porosity of the polymer layer. The dependence of the double layer capacity on the polymerization charge (Fig. 37b) is nearly linear and similar to one, estimated for thin polymer films. The value of the estimated conductivity of polymer layer (Fig. 37c), is between 0.5 and $2 \cdot 10^{-5}\,S \cdot cm^{-1}$. This value is much smaller than the values of the electronic conductance characteristic for polybithiophene and can be accounted for ionic conductance of the polymer layer. However, the effect of the inhomogeneity was not considered in the calculation of this value, and it should be thus interpreted as an average through the entire film thickness. Its growth can therefore be interpreted as a sign for growing porosity of the film.

5.4 Influence of inhomogeneity on the electrochemical behavior of conducting polymer layers.

Many authors [25,64 -*80*] have pointed out the necessity of accounting the inhomogeneity effects by analysis of the impedance spectra of conducting polymers. However, only approximate models, like one with constant phase elements (CPE) [lx,*81*] or with diffusion hindrance, calculated with different from 1/2 value of α [78,79], not allowing quantitativ characterization of inhomogeneity, were proposed up to date. The application of the approach of reflection factors, common in electronic ingineering, allowed to simplify the mathematical treatment considerably and to evaluate an exact solution for inhomogeneous transmission line, which takes into account the dependence of all parameters on the distance from the electrode.

The proposed solution is valid only for cases, for which either the ionic or the electronic resistance is negligible. This condition is fulfilled for the electrodeposited layers of polybithiophene, as can be seen comparing impedance spectra measured on the blank Pt electrode and on the same electrode after the deposition of a polymer layer. The real part of the impedance high frequency limit does not change after the polymer deposition

and therefore represent only the resistance between the tip of the Luggin capillary tube and the polymere interface, not including the resistance of the polymer. Test calculations using the expression for the impedance of a transmission line under consideration of both ionic and electronic resistances [27], having comparable values, show however, that the real part of the impedance of such system does not become zero at high frequencies end and therefore should contribute to the entire high frequency resistance. The absence of such contribution justifies the assumed simplification at least for the case of slightly reduced polymer layers, analyzed in this work.

The choice of a function to describe, how particular parameters depend on the distance from electrode should be made in accordance to the expected character of inhomogeneity. For the case of galvanostatically deposited polybithiophene, the ESM images [30] show a macroscopic structure consisting of conic agglomerates with the base on the electrode and the tip directed into the electrolyte solution, as shown in Fig. 38 in diagram form. The specific effective surface, characteristic diffusion length and specific conductivity should therefore decrease with the distance from the electrode and become zero at the distance equal to the layer thickness. The proposed inhomogeneity function (eqn. 35) exhibits the required behavior over the distance range from x = 0 to x = d. Its form undergoes a wide range of possible alterations by change of only two parameters, having a physical meaning as the scale factor (the value of the function at x=0) and the form factor, controlling the character of decreasing, as in Fig. 40. The use of this function allowed good description of experimental data, as can be seen in Fig. 41.

The number of cross-sections, N, required to provide a quasi-infinite dividing of polymer layer has been estimated as 50 for the case of polybithiophene in slightly reduced state, cf. Fig. 42. The computing time for optimization of parameters describing the impedance spectra are direct proportional to the number of the layers but remain still acceptable for N = 50, when using an optimized for speed CNLS fitting program (LEVM) on the IBM RISC 6000 workstation.

It has been found that the possible simplification of calculations using approximate solution (eqn. 34) is unusable for fitting the impedance spectra for inhomogeneities, taking place in reduced polybithiophene layers (cf. Fig. 43). It should be mentioned,

that some approximate expressions for the impedance of inhomogeneous conducting polymers, described in the literature [76,79], are based on similar assumptions of low inhomogeneity and so their applicability to polymer layers, prepared by common electrodeposition techniques are questionable and should be carefully considered in view of the results obtained using the exact solution.

The proposed mathematical model can correctly describe an inhomogeneous system with all parameters depending on the distance. However, the number of parameters, which can be considered to be inhomogeneous in a polymer layer, is restricted by the applied physical model. For instance, if the effective surface coefficient *f* is considered inhomogeneous, the interface related parameters, such as specific capacitance C_{dl} and charge transfer resistance $R_{ct,}$ have to be independent on the distance from the electrode. Analogous, the apparent diffusion coefficient D and the thermodynamic parameter dE/dc have to be independent on distance in case of an assumption of inhomogeneous characteristic diffusion length *l*. Hence, only the inhomogeneities of the effective interface coefficient *f*, the characteristic diffusion length *l* and the specific polymer resistance ρ have to be analyzed.

The inhomogeneity profiles of the specific effective interface coefficient and the characteristic diffusion length, which allow good fit of the experimental data at all electrode potentials, are presented in Fig. 44. The observed character of the distance dependencies are in a good aggreement with the assumed granular macrostructure of the polymer layer. The decrease of the characteristic diffusion length is followed by slower decrease of the specific effective surface. The possible interpretation of this phenomenon is that polymer agglomerates become smaller with the increasing distance from the electrode and simultaneously diminish its volume fraction, which results the corresponding reducing of the specific interface as the summary effect.

The nature of the resistance, determining the charge/discharge kinetics of the polymer layer, is still not well understood. However, the character of the dependence of this resistance on the distance to electrode (Fig. 45) let assume, that the electronic resistance of polymer agglomerates is the reason for distribution of relaxation times. As can be expected, increasing with the distance porosity and decreasing volume fraction of polymer agglomerates yield increasing resistance of the layer. If the ionic resistance

would be the reason for the distribution, it should be decreasing with the distance from the electrode.

The charge transfer resistance of polybithiophene, evaluated from the fit, almost linearly decreases with the electrode potential in the range between 0.9- 0.45 V, as in Fig. 46a. The potential dependence of this quantity is evidently non Nernstian, which indicates the presence of a complex electrochemical equilibrium on the interface of polybithiophene. The potential dependence of the partial derivative $(dE/dc)_E$, denoted in Fig. 46c, is non Nernstian either, in accordance with the results of coulometric investigations reported in [*82*,*83*]. Accounting of the Donnan equilibrium and the interaction between the ions, incorporated into polymer matrix, could possibly allow to describe the observed potential dependence.

The double layer capacity decreases slightly with the potential (Fig. 46b). The decrease of the concentration of doping ions on the interface with reducing the polymer could be the possible reason for this effect. The apparent diffusion coefficient D also exhibits a slight decrease with the electrode potential, as in Fig. 47b. This fact confirms the observed by many authors [37,38] decrease of the volume of the polymer during reduction, which respectively yields more compact polymer agglomerates in reduced state.

6 Conclusion

In this work the processes involved in recharge of conducting polymers have been investigated by means of various electrical measurement techniques. Conventional methods (cyclic voltammetry, coulometry, potentiometry, potential and current pulse, EIS), EIS on twin electrode and EIS under galvanostatical conditions were applied. The two latter investigation methods were developed in our working group and their application and analysis were performed for the first time during this work.

Two recently published models, connecting the kinetic and thermodynamic parameters relevant to the recharge processes of the polymer layer with its electrical properties, have been used to analyze the experimental data and their applicability for different kind of polymer layers has been discussed.

To account for the inhomogeneity of thick polymer layers, which has been established in some cases, the model of Paasch has been generalized using an approach of an inhomogenous transmission line and was applied to analyze the impedance spectra of polymer layers at different oxidation potentials.

- The impedance measurements during the cyclic recharging of polybithiophene and polypyrrole layers show considerable hysteresis in the potential dependence of the pseudocapacity and the resistance. The comparison of calculated CVs with experimentally measured ones allowed the estimation of the faradaic current for high anodic potentials, which was ascribed for solid state polymerisation and/or overoxidation of polymer.

- In order to estimate the electronic resistance of the polymer separately, impedance measurements on a polymer layer, contacted only on the polymer side, have been carried out. Using an analytical solution for the electrical field in the used twin-electrode configuration, specific electronic conductivity and thickness of the layer could be estimated.

- An analysis of the impedance spectra obtained during the first stages of polybithiophene deposition allowed to observe a transition from a granular 3-D to the

2-D growth of the polymer film. An application of the Ho et al. model for layers of intermediate thickness, prepared at low current densities, could be justified. Polymer layers produced by higher current density has been found to be porous and therefore well matching the considerations of the 2-phase model proposed by Paasch at el. A combined analysis of thick and thin polymer layers assuming the constancy of their thermodynamic properties allowed to estimate the effective interface and the average dimensions of the polymer agglomerates. An increasing inhomogeneity has been observed for polymer layers with growing thickness.

- A model has been developed in order to describe macroinhomogenous polymer layers. The assumption of the polymer as a 2-phase medium with structural parameters, differing in the direction perpendicular to the electrode interface, has been realized using the approach of an inhomogeneous transmission line. Good correspondence of the proposed model to the impedance spectra of polybithiophen, measured at different electrode potentials, has been observed. CNLS fit of experimental data with the model function allowed to estimate thermodynamic and kinetic parameters of the polymer, along with the information about the structure of polymer layer.

7 Acknowledgments

This doctoral thesis is a product of three years I spent inside of a lively and creative working group, which made a considerable contribution to my development as a scientist as well as to my acclimatizing in unusual ethnic surroundings. This group, as I have found it, is a result of long scientific and organizing activity of Prof. R.N.Schindler, whom I am indebted for his credit of trust to invite me for carrying out my Ph.D. research and for an effective help in every scientific and private affairs, which always came in time.

Helpless in the foreign country, I stepped into the office of Dr. Popkirov one good day of 1990, and to my great surprise and relieve conceived the words of my mother language. Since that, George steadily assisted me in all this small practical and theoretical problems, usual in the scientific work, actually forming my attitude to the electrochemistry as to an exact science. I also spent uncountable hours with the unique impedance experimental equipment, which he created. It always allowed to realize even my most wild ideas. And this long discussions with him, where we *always* came to the consensus....I am greatly thankful to him for all this!

Always there with his good advise was Dr. Alexander Kukui, who considerably influenced the formation of my taste to the mathematical analysis and to scientific work in generally. Each time, he found my great mathematical problems "quite simple".

To all my colleagues, who created this indescribable atmosphere of the helpful cheerfulness, I would like to extend my warm thanks. Axel Müller, Mathias Burmeister, Martin Olbrich-Stock, Thorsten Benter, Volker Sauerland, Martin Liesner, Ulf Kirchner - all you made me feel at home at the Institute and helped me to find my way through all imaginable small and big problems. Uwe Eggers and Michael Karstens were responsible for solving the technical ones, which freighted me most. Mr G.Hammerich was the creator of the collection of beautiful glassy measurement equipment, which includes parts I was sure were impossible to prepare. Mr A.Kracht made his contrubution to the electronical equipment I could not dispence in my work.

The hours I did not spent in the Institute during this years was blessed by the sympathy of Rex and Leslie Slate, Lourdes Lemos, the family of Kukui and Sudesha, who made my love to Kiel even deeper. The love of my parents accompanied me since I know me, along with the effective support, which was always as understoodly as the air I breath. Спасибо!

Last but not least I would like to speak out my deep thankfulness to the Gottlieb-Daimler-und-Karl-Benz Stiftung and its staff not only for making possible my research stay in Germany, but also for the feeling to be a part of a big family they gave each participant.

Referent: ...Dr. Georgy Popkirov.....

Korreferent: ...Prof. Schindler.....

Tag der mündlichen Prüfung: ....6/7/1996.....

Zum Druck genehmigt: Kiel, den ..10/7/1996.....

.....

Dekan

Diese Dissertation wurde mit der freundlichen Erlaubnis des Dekans der Mathematisch- Naturwissenschaftlichen Fakultät, Prof. Dr. R. Haensel, in englischer Sprache angefärtigt. Dies wurde nicht durch meine mangelnde Zuneigung zur deutscher Sprache verursacht, sondern vielmehr durch meinen Wunsch, die Ergebnisse meiner Arbeit in Kiel auch meinen russischen und ukrainischen Kollegen zur Verfügung stellen zu können.

8 References

1. H.Shirakawa, E.J. Louis, A.G. MacDiarmid, C.K. Chiang, A.J. Heeger J.Chem.Soc.,Chem.Commum., (1977) 578

2. A. F. Diaz, K. Kanazawa, G. Gardini, J. Chem. Soc. Chem. Commun., 14**,** (1979) 635

3. A. G. MacDiarmid, S.-L. Mu., N. L. Somasiri, and W. Wu, Mol. Cryst. Liq. Cryst., 121**,** (1985) 187

4. T. Kobayashi, H. Yoneyama, and H. Tamura, J. Electroanal. Chem. 161**,** (1984), 187

5. E. W. Paul, A. J. Ricco, and M. S. Wrighton, J. Phys. Chem., 89, (1985) 1441

6. T.B.Hunter, P.S.Tyler, W.H.Smyrl and H.S.White, J.Electrochem.Soc., 134 (1987) 2198.

7. F.Beck and P.Hulser, J.Electroanal.Chem., 280 (1990) 159.

8. M.M.Musiani, Electrochim.Acta, 35 (1990) 1665.

9. J.Tanguy, J.L.Baudoin, F.Chao and M.Costa, Electrochim.Acta, 37 (1992) 1417.

10. R.John and G.G.Wallace, J.Electroanal.Chem., 354 (1993) 145.

11. R.Holze and J.Lippe, Synth.Met., 38 (1990) 99.

12. J.Kruszka, M.Nechtschein and C.Santier, Rev.Sci.Instrum., 62 (1991) 695.

13. R.Bilger and J.Heinze, Synth.Metals, 43 (1991) 2893.

14. A.R.Hillman and M.J.Swann, Electrochim.Acta, 33 (1988) 1303

15. C.Arbizzani and M.Mastragostino, Electrochim.Acta, 35 (1990) 251.

16. G.Morea, C.Malitesta, L.Sabbatini and P.G.Zambonin, J.Chem. Soc.Faraday Trans., 86 (1990) 3769.

17. G.G. Pickup and R.A. Osteryoung, J. Electroanal. Chem., 195 (1985) 271

18. N. Mermiliod, J. Tanguy and F. Petiot, J. Electrochem. Soc.,133 (1986) 1073

19. F. Beck and M. Oberst, Makromol. Chem. Makromol. Symp., 8 (1987) 97

20. S. Panero, P. Prosperi, S. Passerini and B. Scrosati, J. Electrochem. Soc., 136 (1989) 3729

21. S.W.Feldberg, J.Am.Chem.Soc., 106 (1984) 4671

22. T. Yeu, T.V. Nguyen and R.E. White, J.Electrochem.Soc., 135 (1988) 1971

23. T. Yeu, K.M. Yin, J. Carbajal and R.E. White, J. Electrochem.Soc., 135 (1991) 2869

24. D.A. Kaplin and S. Qutubuddin, J. Electrochem. Soc., 140 (1993) 3185

25. J. Tanguy, N. Mermilliod and M. Hocklet, J.Electrochem.Soc., 134 (1987) 795

26. M.A.Vorotyntsev and J.P.Badiali, Electrochim.Acta, 39 (1994) 289

27. G.Paasch, K.Micka and P.Gersdorf, Electrochim.Acta, 38 (1993), 2653

28. G.Schiavon, S.Siran and G. Zotti, Synth. Met., 32, (1989) 209

29. J. Kankare and E.-L. Kupila, J. electroanal. Chem., 322, (1992) 167

30. G.Kossmehl, D.Fechler, W.Plieth, W.-F. Zhang and J.Zerbino, in Werkstoffe in der electrochemnie, Dechema-Monographien- Band 121, 279, VCH Verlagsgeselschaft-Weinheim, Germany (1990)

31. L.Olmedo, I. Chanteloube, A. Germain, M.Petit and E.M.Genies, Synth.Met., 30, (1989) 159

32. A.R. Hillman and E. F. Mallen, J. Electroanal. Chem. 220 (1987) 351.

33. F.Li and W.J.Albery, Electrochim.Acta, 37 (1992) 393.

34. J. Heinze, K. Hinkelmann, M. Dietrich and J. Mortensen, Dechema Monographien, 102 (1986) 209.

35. P. Tschuncky, J. Heinze , Voltammetric Studies on the Electropolymerization Mechanism of Methoxythiophenes , Synth. Met. 55 (1993) 1603.

36. G. Koßmehl, D. Fechler, W. Plieth, W.-F. Zhang, J. Zerbino , Untersuchungen zur Struktur und Morphologie elektrisch leitenderPolymerschichten auf Polythiophen-Basis , DECHEMA-Monogr. 121 (1990) 279

37. A. Hamnett, A. R. Hillman, J. Electrochem. Soc., 135 (1988) 2517.

38. F. Chao, M. Costa, C. Tian , Synth. Met. 53 (1993) 127.

39. G. Tourillon and F. Garnier, J. Phys. Chem., 87 (1983) 2289.

40. G. Schiavon, S. Sitran and G. Zotti, Synth. Metals, 32 (1989) 209.

41. R.Bilger and J.Heinze, Synth.Metals, 43 (1991) 2893.

42. C.K. Baker, J.R. Reynolds , Am. Chem. Soc., Div. Polym. Chem., 28 (1987) 284.

43. G.S. Popkirov aund R.N. Schindler, Ber. Bunsenges.phys.Chem, 97 (1993) 479.

44. J. Roncali, F. Garnier, M. Lemaire and R. Garreau, Synth. Metals, 15 (1986) 323.

45. J. Roncali, M. Lemaire, R. Garreau and F. Garnier, Synth. Metals 18 (1987) 139.

46. B. Zinger, Y. Greenwald, I. Rubinstein, Synth. Metals 41 (1991) 583

47. F. Sundholm, G. Sundholm, M. Törrönen , Synth. Met. 53 (1993) 109.

48. C.Ho, I.D.Raistrick and R.A.Huggins, J.Electrochem.Soc., 127 (1980) 343.

xlix. G.S.Popkirov and R.N. Schindler, Rev. Sci. Instrum. 63/11 (1992) 5366

l. G.S.Popkirov and R.N. Schindler, Electrochim. Acta, 39 (1994) 2025

li. G.S.Popkirov, E.Barsoukov and R.N.Schindler, Electrochimica Acta, 40 (1995) 1857

lii. R.C.Larson, R.T.Iwamoto, and R.N.Adams, Anal. Chim. Acta, 25 (1961) 371

liii. J. E.McClure, D.L.Maricle, Anal. Chem., 39 (1967) 236

liv. S. Fletcher, J.Electroanal.Chem., 337 (1992) 127.

lv. K.J.Binns, P.J. Lawrenson, C.W.Trowbridge "The Analytical and Numerical Solution of Electric and Magnetic Fields", John Wiley & Sons, 1992

lvi J. R. Macdonald, Electrochimica Acta, 35 (1990) 1483.

lvii. J.J.More in G.A.Watson (ed.), Lecture Notes in Mathemiatics: v. 630, Numerical Analysis, Springer-Verlag, Berlin, 1978, p. 105

lviii. O.Genz, M.M.Lohrengel and J.W.Schultze, Electrochim.Acta, 39 (1994) 179.

lix. G.S.Popkirov and E.Barsoukov, J.Electroanal.Chem., 383 (1995) 155.

lx. J.Tanguy, N.Mermilliod and M.Hoclet, J.Electrochem.Soc., 134 (1987) 795.

61. O. Zinke, A.Vlcek, "Lehrbuch der Hochfrequenztechnik", Bd.1, 3., neubearb. u. erw. Aufl. (1987), Springer-Verlag New York Heidelberg Berlin, pp. 60- 64

62. K.Naoi, K.Ueyama, T.Osaka and W.H.Smyrl, J.Electrochem.Soc. 137 (1990) 494.

63. R.M.Penner and C.R.Martin, J.Phys.Chem. 93 (1989) 984. 21. M.M.Musiani, Electrochim.Acta, 35 (1990) 1665.

64. X.Ren and P.G.Pickup, J.Chem.Soc. Faraday Trans., 89 (1993) 321.

65. W.J.Albery, C.M.Elliott and A.R.Mount, J.Electroanal.Chem., 288 (1990) 15.

66. W.J.Albery and A.R.Mount, J.Electroanal.Chem., 288 (1990) 15.

67. J.Heinze, M.Strzbach and J.Mortensen, Ber.Bunsenges. Phys. Chem., 91 (1987) 960.

68. I.Rubinstein, E.Sabatani and J.Rishpon, J.Electrochem.Soc., 134 (1987) 3078.

69. R.S.Hutton, M.Kalaji and L.M.Peter, J.Electroanal.Chem., 270 (1989) 429.

70. J.Heinze, R.Bilger and K.Meerholz, Ber.Bunsenges. Phys. Chem., 92 (1988) 1266.

71. J.Heinze, "Electronic conducting polymers", in "Topics in current chemistry", v.152, Springer-Verlag, Berlin 1990

72. G.P.Evans, "The electrochemistry of conducting polymers", in "Advances in Electrochemical Science and Engineering",Ed.:H.Gerischer and C.W.Tobias, VCH Verlagsgeselschaft GmbH, Weinheim (Germany) 1990.

73. M.Salmon, A.F Diaz., A.J.Logan, M. Krounbi, J. Bargon, Mol.Cryst. Liq. Cryst., 83 (1983) 1297

74. G. Tourillon, Handbook of conducting polymers, Ed. T.A.Skotheim, Marcel Dekker, Inc., 1986, p. 293

75. D. L. Miller and J. O'M. Bockris, J. Electrochem. Soc. 139 (1992) 967.

76. G. La'ng and G. Inzelt, Electrochim. Acta, 36 (1991) 847

77. C. Gabrielli, H. Takenouti, O. Haas and A. Tsukada, J. Electroanal. Chem., 302 (1991) 59.

78. G. Inzelt, G. La'ng, J. Electroanal. Chem. 378 (1994) 39-49.

79. Z. Stoynov, Electrochim. Acta, 35 (1990) 1493

80. M. Edeling, K. Mund, W.Naschwitz, Siemens Forsch. u. Entwickl. Ber. 12 (1983), 85

81. G. La'ng, J. Bacskai and G. Inzelt, Electrochim. Acta, 38 (1993) 773

82. S. Porter, Mat. Sci. Forum. 42 (1987) 43

83. J. H. Kaufman, J. W. Kaufer, A. J. Heeger et al., Phys. Rev. B., 26 (1982) 2327